Characterization of the KRas drug interactions by Limited Proteolysis-Mass Spectrometry and Molecular Dynamics simulations

A thesis submitted to McGill University

In partial fulfillment of the requirements of the degree

Master of Science

Submitted on October 2024 by:

Foroughsadat Absar

Division of Experimental Medicine

McGill University, Montreal

Table of Contents

List of Figures and Tables

List of Abbreviations

AKT - Protein Kinase B

CID - Collision-Induced Dissociation

CPS - Counts Per Second

CRC - Colorectal Cancer

DMSO - Dimethyl Sulfoxide

EGFR - Epidermal Growth Factor Receptor

ERK - Extracellular Signal-Regulated Kinase

FDA - Food and Drug Administration

GAP - GTPase-Activating Protein

GDP - Guanosine Diphosphate

GEF - Guanine Nucleotide Exchange Factor

GTP - Guanosine Triphosphate

GTPase - Guanosine Triphosphatase

G12D - Glycine-to-aspartic acid mutation at position 12 in KRas

HDX - Hydrogen Deuterium Exchange

HTS - High-Throughput Screening

KRas - Kirsten rat sarcoma viral oncogene homolog

LC-MS - Liquid Chromatography-Mass Spectrometry

LiP-MS - Limited Proteolysis-Mass Spectrometry

MAPK - Mitogen-Activated Protein Kinase

MD - Molecular Dynamics

MEK - Mitogen-Activated Protein Kinase Kinase

MTOR - Mechanistic Target of Rapamycin

MS/MS - Tandem Mass Spectrometry

NMR - Nuclear Magnetic Resonance

NSCLC - Non-Small Cell Lung Cancer

PDAC - Pancreatic Ductal Adenocarcinoma

PI3K - Phosphoinositide 3-Kinase

RAF - Rapidly Accelerated Fibrosarcoma (serine/threonine-protein kinase)

RAS - Rat sarcoma viral oncogene homolog

RMSF - Root Mean Square Fluctuation

SDS-PAGE - Sodium Dodecyl Sulfate-Polyacrylamide Gel Electrophoresis

SOS1 - Son of Sevenless homologue 1

TIC - Total Ion Chromatogram

UPLC- Ultra performance Liquid Chromatography

Acknowledgment

I would like to express my sincere gratitude to Dr. Christoph H. Borchers for his unwavering support throughout my master's degree. His guidance has been invaluable during this journey.

I am deeply thankful to Dr. Evgeniy V. Petrotchenko for his patience and insightful guidance. I have learned so much from him on a daily basis.

A special thanks to Danial for his continuous support and for making this path smoother.

I would also like to extend my appreciation to my academic advisor and committee members for their feedback and support: Dr. Michael Witcher, Dr. Horacio Saragovi, and Dr. Hyman M. Schipper.

Finally, I would like to thank my family in Iran for their emotional support and my colleagues Negar, Negin, and Neda for accompanying me throughout this journey.

CHB is grateful for support from the Segal McGill Chair in Molecular Oncology at McGill University (Montréal, Quebec, Canada). CHB is also grateful for support for the Segal Cancer Proteomics Centre at the Jewish General Hospital (Montréal, Quebec, Canada) from Genome Canada and Genome Quebec via the MutaQuant GAPP (#6567 Borchers_Zahedi_APF), and from the Terry Fox Research Institute and the Alvin Segal Family Foundation. CHB is also grateful for support for the Warren Y. Soper Clinical Proteomics Centre at the Jewish General Hospital (Montréal, Quebec, Canada) from the Warren Y. Soper Charitable Trust.

Contribution of Authors

In accordance with McGill Guidelines, the candidate chose to present the results of this thesis in a manuscript-based format. This thesis was written by Foroughsadat Absar, who was responsible for drafting the Limited Proteolysis-Mass Spectrometry part of the manuscript and preparing the visual data representations. Foroughsadat Absar was entirely responsible for conducting the literature review in Chapter 1. She also designed all the mass spectrometry related experiments, conducted them, analyzed the data, and interpreted the results presented in Chapter 2. Christoph H. Borchers provided overall supervision, offering guidance and feedback throughout the process. Both Evgeniy V. Petrotchenko and Christoph H. Borchers supervised the experimental procedures and assays, contributing valuable insights during the execution of the experiments. The inhibitors mentioned in the experiments were kindly provided by Edith Nagy, Jason B. Cross, and Roopa Thapar of University of Texas, MD Anderson Cancer Center.

The manuscript's section on molecular dynamics simulations was written by Brandon Novy. The simulations themselves were conducted by Brandon Novy and Konstantin I. Popov of the University of North Carolina at Chapel Hill, in collaboration with Borchers' laboratory. Foroughsadat Absar interpreted these simulations and integrated the molecular dynamics results with the findings from the LiP-MS experiments, enhancing the overall analysis presented in the manuscript.

Abstract

An important step in high throughput screening of small-molecule libraries for drug discovery is the prioritization and validation of "hits" to rule out false positives. This is usually done by using biochemical or binding assays. The development of orthogonal assays that are highly sensitive can accelerate the hit-to-lead process. These assays differ from the primary assays and are valuable in small-molecule screening. Limited proteolysis combined with mass spectrometry (LiP-MS) is an informative technique for studying changes in protein structure upon ligand binding. LiP-MS utilizes short-duration exposure of proteins under native conditions to low concentration of proteases. The resulting proteolytic pattern is sensitive to the structure of the protein at the cleavage site, and this structure can change upon ligand binding. Here, we have characterized the interaction of published small molecule inhibitors with the KRas G12D mutant oncoprotein by LiP-MS. We used intact protein mass spectrometry and top-down analysis to detect and identify KRas G12D cleavage products in the presence and absence of inhibitors, which allowed us to locate the cleavage sites within the protein sequence. Cleavage sites protected after drug binding correspond to the location of the drug binding site.

The limited proteolysis yield could be estimated quantitatively using intact protein mass spectrometry, and we found that the degree of cleavage depended on both the binding affinity and the presence of specific functional groups in the inhibitor structure. A comparison of molecular dynamics simulations for the drug-free and drug-bound protein revealed the atomistic mechanisms by which the cleavage sites, located in flexible and disordered protein regions, are stabilized upon drug binding. Analysis of the interaction patterns throughout the simulation for

each protein-ligand complex corroborated the changes in protein dynamics, and correlated well with shifts in the experimentally derived proteolysis yields.

This study demonstrates that this approach can be used to identify target sites within protein sequences that are important for protein-ligand interactions, as well as allowing the characterization and ranking of ligands with different binding affinities. These capabilities make LiP-MS a valuable tool in small molecule screening studies and demonstrate that it can be a potential addition to traditional methods for high-quality “hit” selection in the early stages of drug discovery.

Résumé

Une étape importante dans le criblage à haut débit de bibliothèques de petites molécules pour la découverte de médicaments est la priorisation et la validation des "hits" afin d'éliminer les faux positifs. Cela est généralement réalisé à l'aide de tests biochimiques ou de liaison. Le développement de tests orthogonaux hautement sensibles peut accélérer le processus de passage des hits aux leads. Ces tests, différents des tests primaires, sont précieux dans le criblage de petites molécules. La protéolyse limitée combinée à la spectrométrie de masse (LiP-MS) est une technique informative pour étudier les changements de structure des protéines lors de la liaison avec un ligand. La LiP-MS utilise une exposition de courte durée des protéines, dans des conditions natives, à une faible concentration de protéases. Le motif protéolytique résultant est sensible à la structure de la protéine au site de clivage, qui peut changer lors de la liaison d'un ligand. Dans cette étude, nous avons caractérisé l'interaction d'inhibiteurs de petites molécules avec l'oncoprotéine mutante KRas G12D par LiP-MS. Nous avons utilisé la spectrométrie de masse des protéines intactes et une analyse top-down pour détecter et identifier les produits de clivage de KRas G12D en présence et en absence d'inhibiteurs, localisant ainsi les sites de clivage dans la séquence protéique. Les sites de clivage protégés lors de la liaison des médicaments correspondaient à l'emplacement du site de liaison du médicament. Le rendement de la protéolyse limitée a pu être estimé quantitativement grâce à la spectrométrie de masse des protéines intactes, et nous avons constaté que le degré de clivage dépendait à la fois de l'affinité de liaison et de la présence de groupes fonctionnels spécifiques dans la structure de l'inhibiteur. Une comparaison des simulations de dynamique moléculaire pour la protéine libre et la protéine liée au médicament a révélé les mécanismes atomistiques par lesquels les sites de clivage, situés dans des régions flexibles et désordonnées des protéines, sont stabilisés lors de la liaison du médicament.

L'analyse des motifs d'interaction tout au long de la simulation pour chaque complexe protéine-ligand a corroboré les changements dans la dynamique des protéines, et a montré une bonne corrélation avec les variations des rendements de protéolyse obtenus expérimentalement. Nous démontrons que cette approche peut être utilisée pour identifier des sites cibles dans les protéines importants pour les interactions protéine-ligand, ainsi que pour caractériser et classer les ligands avec différentes affinités de liaison. Ces capacités font de LiP-MS un outil précieux dans les campagnes de criblage de petites molécules et un ajout potentiel aux méthodes traditionnelles pour une sélection de haute qualité des "hits" dans les premières étapes de la découverte de médicaments.

Chapter 1: General Introduction and Literature Review

1. Protein-small molecule interactions

The characterization of protein-small molecule interactions is of considerable interest because small molecules continue to be indispensable for the drug-discovery industry, due to their diverse applications and adaptability.(1) In order to efficiently utilize small molecules in drug discovery, it is important not only to understand their interactions with proteins but also to systematically prioritize potential hits and validate them during the screening process. An important step in high-throughput screening (HTS) is hit prioritization and validation. These steps typically involve biochemical or binding assays.(2) Biochemical assays often use purified target proteins and measure either their binding to ligands or the inhibition of enzymatic activity *in vitro*.(3) These assays are frequently conducted using "competition" formats, where the compound under study displaces a known ligand or substrate. These compounds are normally quantified through methods such as absorbance, fluorescence, or luminescence.(4) Binding assays are also commonly used to validate hits. This validation is done by detecting the direct interaction of library components with the target protein. This process is more valuable in the later phases of the drug discovery process, such as during hit validation and optimization.(5) These primary assays – i.e., biochemical and binding assays -- can be susceptible to various forms of interference. Unlike the mentioned methods, orthogonal assays provide a highly sensitive approach to confirming the true activity of compounds. These assays are designed to be different from the primary assays as they focus on alternative detection mechanisms or conditions, and this helps to decrease assay artifacts and reduce false positives. Mass spectrometry (MS)-based assays are a form of orthogonal assay., MS-based assays are widely regarded for their sensitivity and accuracy, and MS-based orthogonal

assays can detect direct interactions between small molecules and target proteins.(6) Moreover, orthogonal assays utilizing mass spectrometry can be more reliable in the detection of target engagement than traditional biochemical assays, because those other methods may be prone to interference from compounds that affect assay readout through unrelated mechanisms including fluorescence quenching or aggregation.(7) Given the high sensitivity and specificity of mass spectrometry in detecting true compound activity and minimizing assay artifacts, various methods based on this technology have been developed to improve the drug discovery processes. One such approach is limited proteolysis coupled with mass spectrometry (LiP-MS). LiP-MS is a robust technique that provides deep insights into protein structural changes upon ligand binding.

2. Limited Proteolysis- Mass Spectrometry

2.1. Limited Proteolysis- Mass Spectrometry technique

Limited proteolysis combined with mass spectrometry (LiP-MS) is an informative technique for studying changes in protein structure upon ligand binding. In this method, a proteolytic enzyme is used to cleave the protein into fairly large particles, during a short exposure time. Considering the speed of the cleavage in this method, the first cleavage occurs while the three-dimensional structure (tertiary structure) of the protein and the arrangement of the subunits (quaternary structure) are still preserved. Thus, the accessibility of a specific residue to cleavage determines the cleavage product, and this accessibility can be affected by three factors: the protein structure, the specificity of the proteolytic enzyme, and the size of the enzyme.(8) In nature, proteins fold

with hydrophobic regions on the inside and hydrophilic regions on the outside. Proteases preferentially cleave surface-exposed regions, especially disordered regions or loops, while well-folded regions resist cleavage. When a small molecule binds to a protein, the proteolytic accessibility of the enzyme to the protein can be changed, resulting in a change to its LiP pattern. Small-molecule binding stabilizes the protein structure, resulting in fewer exposed cleavage sites. Comparing the LiP patterns of proteins in the presence and the absence of the ligand, and thereby determining the regions of the protein surface that are protected from limited proteolysis, can identify the sites of the protein-small molecule interactions.(9)

Different broad-specificity proteases can be used for LiP.(10-13) Proteinase K is frequently used as the proteolytic enzyme in limited proteolysis experiments. This enzyme is known for its broad specificity and efficiency. Its ability to cleave at different sites and work effectively under various conditions enables a comprehensive analysis of protein structure and dynamics.(10-12) Chymotrypsin is another enzyme that can be used for limited proteolysis. This proteolytic enzyme is broadly specific with a preference for hydrophobic residues.(12, 13) Hydrophobic residues are typically buried in the protein globule in the native folded state. Upon structural rearrangement of a protein, surface exposure of specific amino acid residues within a protein can change due to the change in conformation. The regions of the protein structure that are normally buried inside the protein can become more exposed and therefore more accessible to proteolytic enzymes. Thus, proteolytic enzymes such as chymotrypsin with a cleavage tendency towards the hydrophobic residues, are useful for the differential detection of such changes.(14-16)

The size of the proteolytic enzyme used for limited proteolysis is another factor affecting the cleavage products. Most proteolytic enzymes used for this procedure are medium-sized globular proteins with molecular weights of at least 15-20 kDa. Thus the location of the cleavage sites

reflects the accessibility of these sites to a spherical protein whose diameter corresponds to the size of the enzyme used.(17)

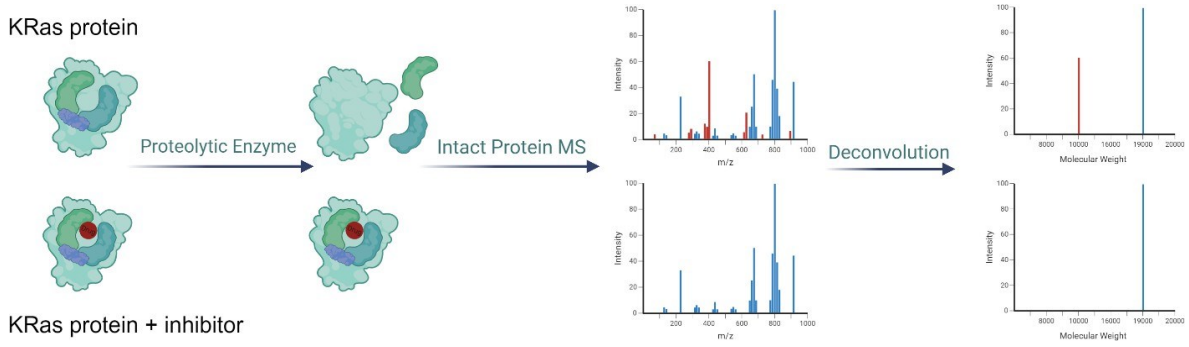

Figure 1. Limited Proteolysis Mass Spectrometry (LiP-MS) Workflow for KRas Analysis.

The figure illustrates how LiP-MS is used to compare the proteolysis patterns of KRas protein in the presence and absence of an inhibitor. When the inhibitor binds, it stabilizes the protein structure, resulting in fewer cleavage sites. The mass spectrometry results highlight these changes, allowing the identification of protected regions and providing insights into protein-ligand interactions.

The next step is the determination of the actual limited-proteolysis cleavage sites. The conventional approach to performing a limited-proteolysis reaction is to characterize the cleavage products through a combination of gel separation using sodium dodecyl sulfate-polyacrylamide gel electrophoresis (SDS−PAGE) and mass spectrometry.(18) Typically, a series of time points is used to monitor the progression of the cleavage (e.g., 1−5 min exposures of the protein to a proteolytic enzyme at a 1:100 enzyme/substrate ratio), and the gel bands obtained from the SDS−PAGE

separation in this process are analyzed using in-gel digestion and peptide mapping to identify the actual cleavage sites.(19) Fourier-transform mass spectrometry for larger molecules has made it possible to use top-down mass spectrometry combined with tandem mass spectrometry (MS/MS), enabling direct analysis of intact proteins. This allows high-resolution determination of the protein's molecular weight and detailed mapping of the cleavage sites by isolating and dissociating molecular ions.(20)

2.2. Limited Proteolysis- Mass Spectrometry applications

Due to the broad applications of LiP-MS, this method is gaining attention across various research fields. Like traditional proteomic methods, it can be used for the analysis of protein abundance changes caused by different experimental conditions. In addition, LiP-MS can detect structural changes across an entire proteome, which complements the abundance data and, therefore, significantly increases the amount of information obtained from proteomic studies. This makes LiP-MS a powerful tool for functional proteomics. This method can be used to systematically study how cells and organisms respond to environmental, chemical, or genetic changes, and to identify alterations in cellular processes or functions.(21) As an example, this method has been used to assess the structural features of more than 1000 yeast proteins and to detect changes in protein conformations due to changes in nutrients.(10)

LiP-MS is also becoming an important tool in structural biology. It helps to monitor structural changes in thousands of proteins in their complex cellular environments and can identify specific structural alterations, such as small-molecule binding, with the resolution of a single functional site.(21, 22) When combined with other high-resolution techniques such as NMR spectroscopy or

X-ray crystallography, LiP-MS can connect *in-vitro* protein structures to *in-vivo* analyses. By comparing proteolytic patterns from *in-vitro* experiments -- where protein structures are known in detail -- with patterns from the native environment, researchers can draw conclusions about the structural state of proteins *in-situ*.(10, 21) LiP-MS has also been applied to the study of proteome-wide structural changes, where it helps detect alterations in protein conformation across complex proteomes(9, 21). LiP-MS is also used for epitope mapping, where it identifies regions where antigens bind to antibodies(23). LiP-MS has also been applied to the study of prions where it was used to map structural changes that occur during the conversion of prion proteins from their native form to pathogenic oligomers, giving insights into prion-related diseases.(24)

In systems biology, LiP-MS can be used to study protein interactions with small molecules and it also has the potential for studying protein-protein interactions, as shown in research on chaperone-client interactions.(21, 22, 25) The LiP-MS technique could also be expanded to explore global interactions between proteins and biopolymers such as DNA, RNA, and lipids. LiP-MS is also being used to study metabolite-protein interactions, revealing known and novel relationships in cells.(25, 26)

In addition, the high-throughput capacity of the optimized LiP-MS protocol makes it useful for translational research, including drug-target identification and screening for new disease biomarkers based on structural changes of proteins.(22, 27) LiP-MS has also been used to deconvolute drug targets directly in human cells at the proteome-wide level. It also enabled the investigation of protein-small molecule interactions, identifying drug targets and their binding sites, thus enabling the study of interactions in the native cellular environments.(9, 22) LiP-MS can also be useful for predicting the binding of small-molecules to proteins, helping with drug discovery by identifying binding sites. LiP-MS is also useful for profiling structure-based target

engagement in drug discovery, helping researchers understand how drugs interact with their targets at a molecular level.(28)

LiP-MS has been used to determine the thermostability of the complete proteomes of human cells and *Escherichia coli*, providing insights into protein stability and thermally induced unfolding.(11) It also has been used for measuring the refolding efficiency of proteins (29).

Table 1 outlines key applications of LiP-MS, including functional and structural proteomics, systems biology, and drug target identification.

Application Type	Example of Application	References
Functional Proteomics	Study of cellular response to environmental or genetic changes, including analysis of the structural changes of more than 1000 yeast proteins upon nutrient shifts	**(10,21)**
Structural Biology	Monitoring structural changes in proteins and small molecule binding, including detection of alterations in protein conformation across complex proteomes, epitope mapping (identification of regions of the antigen regions bound to antibodies), and Characterization of structural changes of the prion protein during conversion to pathogenic oligomers	**(9,10,21,22, 23, 24)**
Systems Biology	Study of protein interactions with small molecules and biopolymers, including metabolite-protein interactions and protein-protein interactions	**(21, 22, 25, 26)**
Drug Target Identification	Deconvolution of drug targets in human cells, including prediction of small molecule binding sites for drug discovery and structure-based target engagement profiling	**(9, 22, 27, 28)**
Other Applications	Study of thermostability in human and *E. coli* proteomes, and measuring protein refolding efficiency	**(11, 29)**

Table 1. Summary of LiP-MS Applications in Proteomics and Related Fields.

3. KRas

3.1. KRas Signaling Pathway

KRas, a member of the RAS gene family, encodes a protein that plays an important role in cell-signaling pathways regulating cell growth, proliferation, differentiation, and survival. KRas normally acts as a molecular switch, activating downstream pathways when GTP is bound, but inactive when GDP is bound. The active, GTP-bound form of KRas has been described as a "coiled spring" which in turn activates effector proteins such as RAF1, BRAF, or PI3K, activating the RAF/MEK/ERK or PI3K/AKT/MTOR cascades, respectively.(30)

KRas exists in two isoforms, KRas-4A and KRas-4B. KRas-4B is more commonly associated with human cancers. KRas-4A needs to be palmitoylated to facilitate its movement from the endoplasmic reticulum to the plasma membrane, but KRas-4B does not rely on palmitoylation. Instead, KRas-4B attaches to the plasma membrane through farnesylation, with a polybasic lysine-rich region near the C-terminal cysteine, which anchors it to the negatively charged membrane lipids.(31, 32)

When epidermal growth factor (EGF) binds to its receptor (EGFR), wild-type KRas becomes activated, triggering a cascade of intracellular signals.(33) This activation is a result of exchanging GDP for GTP. This process is facilitated by guanine nucleotide exchange factors (GEFs) such as SOS1 (Son of Sevenless homologue 1), which converts inactive GDP-bound KRas into its active GTP-bound KRas. Conversely, GTPase-activating proteins (GAPs) promote the hydrolysis of GTP-bound KRas back to its inactive GDP-bound state.(34, 35)

KRas mutations disrupt the GDP-GTP cycle which impairs the ability of GAPs to hydrolyze GTP. For instance, mutations at codon 12, such as G12D and G12V, significantly reduce the intrinsic GTPase activity, resulting in the accumulation of the active GTP-Bound KRas, and this results in uncontrolled cell growth and proliferation. Each mutation has unique effects on the intrinsic nucleotide exchange and GTP hydrolysis rates.(36, 37)

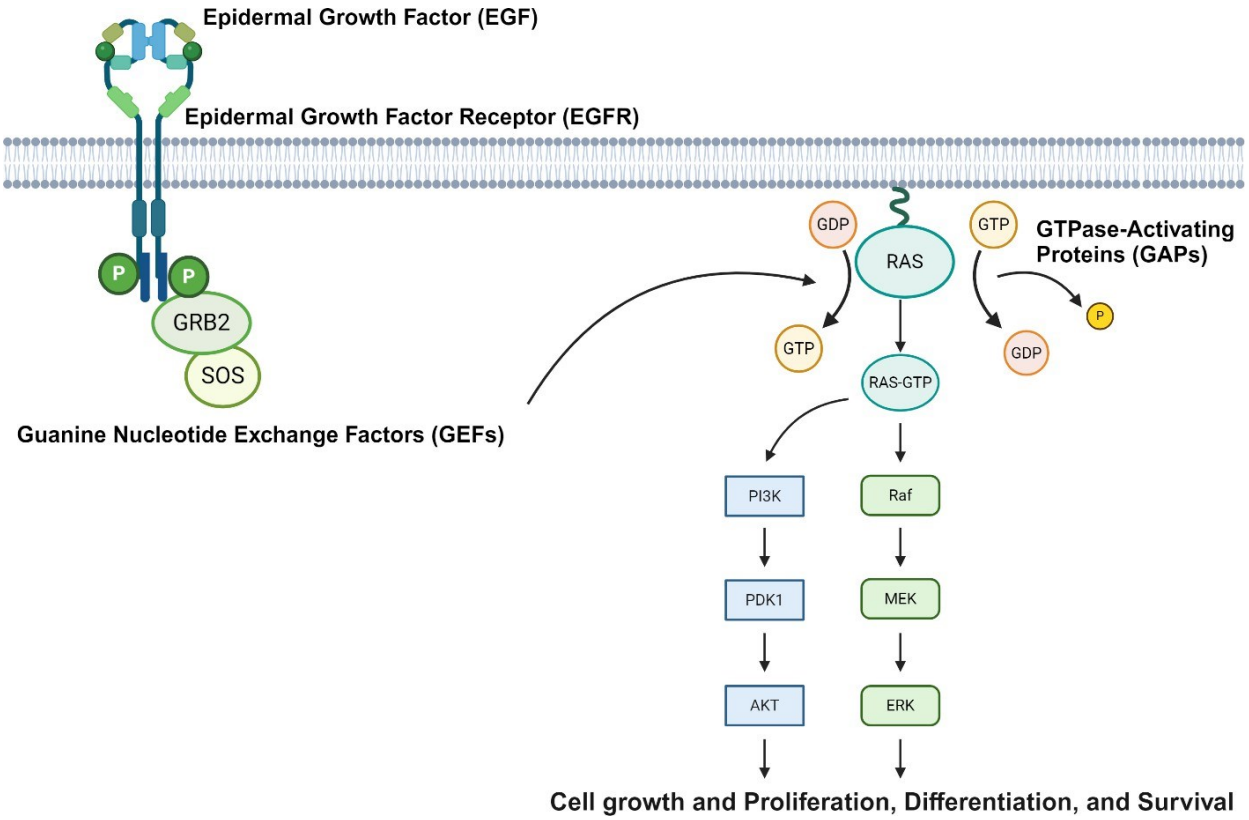

Figure 2. KRas Activation and Signaling Pathways.

KRas acts as a molecular switch in cell signaling pathways regulating growth and survival. Upon EGF binding to EGFR, KRas is activated by GEFs exchanging GDP for GTP, triggering downstream RAF/MEK/ERK and PI3K/AKT pathways. GAPs subsequently inactivate KRas by promoting GTP hydrolysis.

3.2. Epidemiology and Impact of KRas G12D in Different Cancer Types

Mutations in KRas are among the most common oncogenic drivers in human cancers. As mentioned earlier, these mutations cause an increase in GTP-bound KRas levels, leading to more activation of downstream pathways and the subsequent uncontrolled cell growth and tumor development.(38) Activating mutations are most commonly found in single nucleotide substitutions in four "hotspot" codons – 12, 13, 61, and 146. Codon 12 is the most frequently mutated of all four hotspot codons, with the G12D mutation being generally the most prevalent.(39) KRas G12D is the most common mutation (44%) associated with pancreatic ductal adenocarcinoma, which is distinguished by one of the highest mortality rates among all malignant diseases. (40, 41) In pancreatic adenocarcinoma, the KRas G12D mutation is associated with worse overall survival compared with wild-type KRas.(42) This mutation also occurs in approximately 10–12% of colorectal cancer cases, which is the third most deadly cancer worldwide.(43) In colorectal cancer patients, KRas mutations are a predictor of resistance to anti- epidermal growth factor receptor (EGFR) therapy and are associated with a poor prognosis. (44) In non-small cell lung cancer (NSCLC), the prevalence of the KRas G12D mutation is relatively low, occurring in approximately 4% of cases, whereas the G12C variant is more frequent.(39, 45) In NSCLC patients, KRas-G12D mutation causes immunosuppression and enhances resistance to immune checkpoint inhibitors.(46) The high prevalence and poor prognosis associated with KRas G12D mutations in various cancers makes it an attractive target for drug design. Targeting oncogenic KRas proteins could potentially improve treatment outcomes and survival rates for patients suffering from these aggressive malignancies.

3.3 Direct and Indirect Strategies for Targeting KRas

There have been different strategies to target KRas either directly or indirectly including targeting nucleotide exchange, targeting the Ras pathway, generating inhibitors of KRas dimerization, etc.(47)

3.3.1 Targeting nucleotide exchange

One of the approaches for inhibiting KRas is through blocking nucleotide exchange, by targeting the SOS1-KRas interaction. One of the small-molecule inhibitors that effectively disrupts this interaction is BAY-293. This inhibitor specifically binds to the SOS1 protein and prevents it from facilitating the exchange of GDP for GTP on KRas. BAY-293 has demonstrated significant antiproliferative activity in preclinical models, by keeping KRas in its inactive GDP-bound state,(48) BI-3406 is another notable inhibitor that functions similarly, by inhibiting SOS1-mediated KRas activation. This also results in significant tumor growth suppression in KRas-driven models. Additionally, BI-1701963 has emerged as an effective SOS1 inhibitor and is currently being studied for its ability to block KRas activation by maintaining it in its inactive state.(49)

These inhibitors show the potential of targeting nucleotide exchange as an effective strategy for inhibiting KRas activity in cancer. However, one of the limitations of this method is the compensatory mechanisms loops that may diminish the efficacy of SOS1 inhibitors over time, i.e., ERK-mediated feedback.(49)

3.3.2 Targeting the Ras Pathway

One of the strategies to target the Ras pathway is to target the tyrosine kinase receptors (i.e., the EGFR family) and the Ras effector pathways (i.e., MAPK and PI3K).

The EGFR-targeting monoclonal antibodies cetuximab, and panitumumab, combined with standard chemotherapy, have become critical components of treatment regimens for advanced colorectal cancer.(50) However, because mutations in KRas can activate the signaling pathway independently of EGFR, the effectiveness of these therapies can be compromised.(51) As a result, validation of Ras wild-type status is crucial before adding cetuximab or panitumumab to therapy.(52)

Another strategy to target the Ras pathway is through inhibition of downstream effector pathways such as MAPK and PI3K. Inhibiting the pathway, particularly through MEK inhibitors, has shown potential in treating KRas-mutant cancers. However, compensatory signaling through the PI3K pathway can lead to resistance to these therapies. To overcome this, dual inhibition strategies targeting both MEK and PI3K have been explored. Preclinical studies have shown that combining MEK inhibitors like selumetinib with PI3K inhibitors such as BEZ235 can induce greater tumor suppression than single-agent therapy. While dual inhibition is promising, achieving sustained tumor regression remains a challenge, as tumors frequently adapt through alternative signaling pathways.(53)

3.3.3 Inhibitors of KRas dimerization

Ras proteins can form dimers on membrane surfaces, a process known as Ras dimerization. This process enhances their ability to scaffold and activate downstream signaling pathways (54, 55). The α4–α5 interface plays a key role in RAS dimerization and can be targeted to disrupt this process. Recent studies show that small-molecule inhibitors, such as NS1, can bind to this interface and inhibit RAS dimerization, which prevents downstream signal activation.(56) These inhibitors do not alter RAS's GTPase activity or membrane localization, but they hamper its ability to dimerize by binding to the α4–α5 interface, which is crucial for activating key signaling pathways like MAPK.(56, 57)

3.3.4 Target KRas directly

In 2013, Ostrem et al. developed a novel strategy to target the reactive cysteine-12 (Cys-12) in the common KRas G12C mutant, using covalent inhibitors.(58) They identified ARS-1620, a highly potent small-molecule inhibitor that covalently binds to Cys-12 in the switch-II pocket of KRas G12C. This binding does not affect wild-type KRas but alters the nucleotide preference to favor GDP over GTP.(58) ARS-1620 demonstrated significant activity against KRas G12C tumors *in vitro* and *in vivo*.(59) This discovery marked a milestone in targeting mutant KRas, which had long been considered "undruggable." Using this approach, Amgen developed a highly potent and selective KRas G12C inhibitor called AMG510, also known as sotorasib (Lumakras™), which entered Phase I/II clinical trials in 2018 (NCT03600883).(60) The U.S. Food and Drug Administration (FDA) granted accelerated approval to sotorasib in May 2021 based on significant

antitumor activity and manageable side effects in heavily pretreated patients with non-small cell lung cancer (NSCLC) harboring KRas G12C mutations. This approval represents a breakthrough in KRas targeted therapy.(61)

Meanwhile, further research efforts have led to the development of pan-KRas inhibitors such as BI-2865 and BI-2493, designed to target a broader range of KRas mutations beyond G12C, including G12D, G12V, and others. These inhibitors bind non-covalently to the inactive form of KRas and inhibit nucleotide exchange, thereby blocking KRas reactivation and signaling in a wide range of KRas-driven cancers.(62)

The successful development of KRas G12C-specific inhibitors provides valuable insights and inspiration for developing small-molecule inhibitors targeting KRas G12D. In 2021, Mirati developed a potent and selective non-covalent KRAS G12D inhibitor called MRTX1133.(63) Recent preclinical studies have shown promising results, suggesting that MRTX1133 could potentially shift the paradigm in Pancreatic Ductal Adenocarcinoma (PDAC) treatment.(64) This inhibitor binds to GDP-bound KRas G12D in switch-II binding pocket with picomolar affinity and has entered Phase I/II clinical trials.(65)

Recently, a novel covalent approach targeting KRas G12D through strain-release alkylation was introduced. Malolactone-based inhibitors selectively target KRas G12D by forming stable covalent complexes, effectively inhibiting KRas G12D-driven cancer cell proliferation and tumor growth in preclinical models.(66)

Table 2 outlines major milestones in the development of direct KRas inhibitors, from the discovery of KRas mutations to recent advancements in targeting various KRas mutations with both covalent and non-covalent inhibitors, including FDA-approved therapies and ongoing clinical trials.

Year	Milestone	Description	References
1980s	**Discovery of KRas mutations**	KRas identified as a key oncogene driving tumor formation.	**(67)**
1990s	**Early attempts to target KRas**	Initial unsuccessful attempts to develop KRas inhibitors due to its "undruggable" nature.	**(68)**
2013	**ARS-1620**	Ostrem et al. discovered ARS-1620, a covalent inhibitor specifically targeting KRas G12C.	**(58)**
2018	**Sotorasib (AMG 510)**	Amgen's sotorasib enters Phase I/II clinical trials as a covalent KRas G12C inhibitor, the first KRas inhibitor to show clinical efficacy.	**(69)**
2021	**FDA approval of Sotorasib**	Sotorasib becomes the first FDA-approved drug to target KRas G12C mutations in NSCLC.	**(70)**
2022	**Pan-KRAS inhibitors development (BI-2855, BI-2493)**	Pan-KRAS inhibitors targeting multiple KRas mutations (e.g., G12D, G12V, G12C) show promise in preclinical studies, focusing on non-covalent mechanisms.	**(62)**
2022	**MRTX1133**	Mirati develops MRTX1133, a potent and selective non-covalent KRas G12D inhibitor,	**(63)**

		which shows promising results in preclinical studies.	
2023	**MRTX1133 enters clinical trials**	MRTX1133 enters Phase 1/2 clinical trials, advancing efforts to target KRas G12D-driven tumors.	**(71)**
2024	**Covalent G12D inhibitor (Malolactone-based)**	A covalent KRas G12D inhibitor utilizing strain-release alkylation was developed, showing selective targeting of the G12D mutant and effective suppression of tumor growth in preclinical studies.	**(66)**

Table 2. Key Milestones in Direct KRas Inhibitor Development.

4 Molecular Dynamics Simulations

As described above, KRas G12D plays a significant role in cancer. Given the available inhibitors developed for this target, we evaluated the use of Limited Proteolysis-Mass Spectrometry (LiP-MS) in proof-of-concept experiments for the KRas G12D protein. Using intact protein mass spectrometry, we identified KRas cleavage products and used top-down analysis to locate the cleavage sites within the protein sequence.

To complement these findings, we performed molecular dynamics (MD) simulations to get atomic-level insights into protein-ligand interactions, and to see how ligand binding affects KRas stability and conformation.(Figure 3) MD simulations provide a dynamic view of these interactions, offering a more realistic perspective than the static predictions of docking studies. Recent studies have employed molecular dynamics (MD) simulations to elucidate the binding mechanisms of MRTX1133 to KRas G12D. Issahaku et al. characterized MRTX1133's binding to KRas G12D, providing insights into potential inhibitors for cancer therapy.(72) Tu et al. utilized MD simulations and Markov state models to detail the pathways and mechanisms of MRTX1133 binding to KRas G12D.(73) Similarly, Liang et al. investigated the inhibition mechanism of MRTX1133 on KRas G12D through MD simulations and Markov state models.(74) These studies underscore the utility of MD simulations in understanding protein-ligand interactions, complementing experimental techniques like LiP-MS. This combined approach of mass spectrometry and MD simulations has previously revealed spatial organization, metal-binding sites, and protein-ligand interactions in studies on proteins such as metallothionein.(75-79) Integrating LiP-MS with MD simulations helped us validate and refine our understanding of the interactions we studied. Docking studies are a powerful and affordable way to find potential chemical leads by virtually placing small molecules into predicted binding sites. However, they

only provide static images of possible interactions. These studies depend on structural data, such as crystal structures or NMR, to predict how a ligand might fit into a protein's active site.(80)

We can achieve a more comprehensive understanding of protein-ligand interactions by combining docking studies with the dynamic insights from MD simulations and experimental validation from LiP-MS.

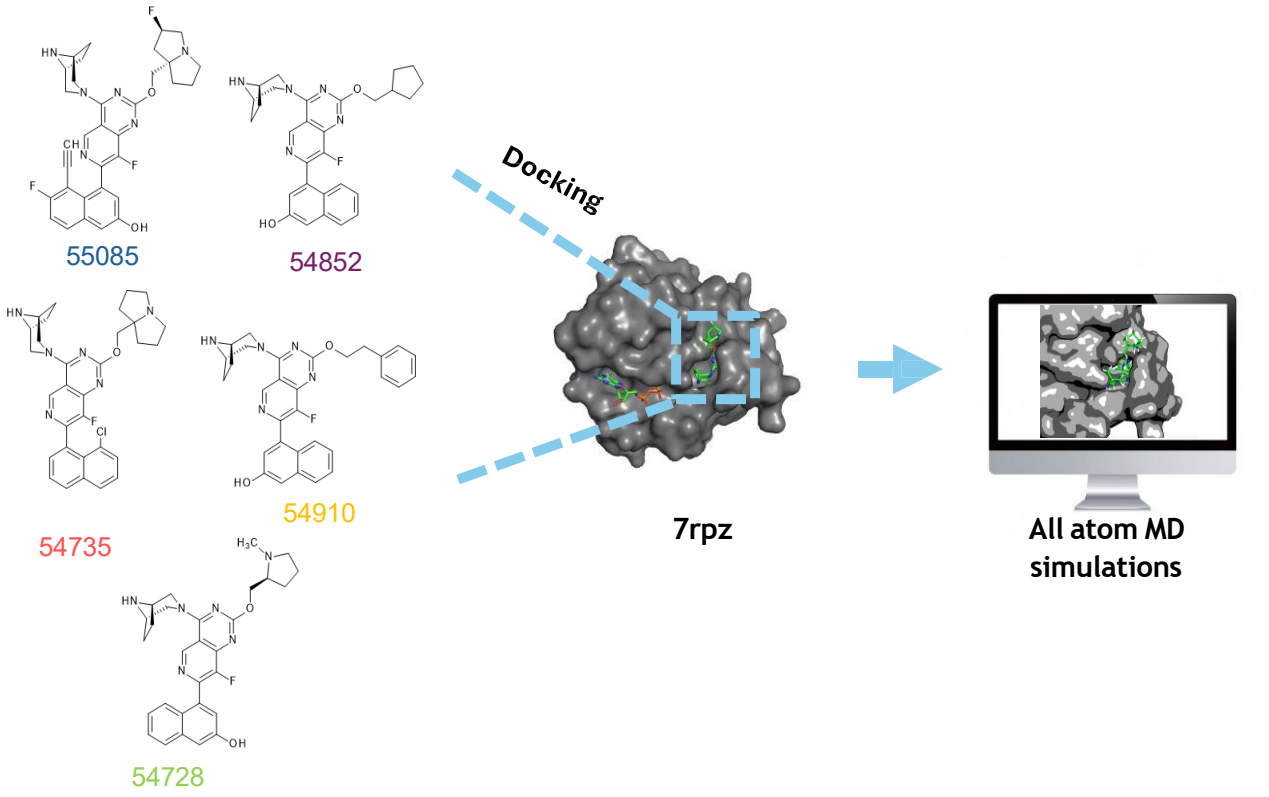

Figure 3. Docking and Molecular Dynamics Simulations of Ligand Binding to KRas (7rpz). Selected small molecules were docked into the KRas 7rpz structure to predict binding interactions. These docking results were further refined and validated using all-atom molecular dynamics (MD) simulations to observe the stability and conformational changes of ligand binding over time.

5. Hypothesis and Objectives

5.1 Hypothesis

We hypothesized that the combination of Limited Proteolysis-Mass Spectrometry (LiP-MS) and molecular dynamics (MD) simulations would provide detailed insights into the binding mechanisms of KRas G12D inhibitors. Specifically, we expected that this integrated approach would identify key ligand binding sites, and would predict how structural changes that occurred upon drug binding would stabilize the flexible regions of the KRas G12D protein and would correlate with proteolysis patterns. This could further assist in the prioritization of compounds in drug discovery efforts by revealing how variations in compound structure and binding affinity influence protein-ligand interactions.

5.2 Objectives

The primary objective of this study was to investigate the interaction of non-covalent KRas G12D inhibitors with the KRas G12D oncoprotein using a combined approach of LiP-MS and MD simulations. Through this approach, we aimed to (i) map ligand binding sites and conformational changes in KRas G12D that occurred upon drug binding, (ii) to correlate proteolytic protection with binding affinities, and (iii) to demonstrate the utility of LiP-MS and MD simulations for hit prioritization and optimization in structure-based drug discovery.

Chapter 2: Characterization of the KRas drug interactions by Limited Proteolysis-Mass Spectrometry and Molecular Dynamics simulations

1. Introduction

Limited proteolysis combined with mass spectrometry (LiP-MS) is an informative technique for studying changes in protein structure. In this method, a non-specific proteolytic enzyme is used to cleave the protein under a short exposure time. The first cleavage event occurs while the protein's tertiary and quaternary structures are preserved. This method is of interest in various applications due to its ability to explore protein interactions under different conditions. It has been widely used to study protein conformational changes, small molecule binding events, and protein-protein interactions.(1-8) This makes LiP-MS particularly valuable in fields such as functional and structural proteomics, as well as drug discovery, where it helps identify binding sites and monitor target engagement.(2, 3, 8-10)

Here, we have used LiP-MS to characterize the mode of binding of five non-covalent Mirati MRTX1133 family drug scaffolds that have recently been developed and which are specific to the KRas G12D oncoprotein.(11) We quantitatively compared the abundance of a single cleavage product between the free and drug-bound protein states, making the LiP-MS part of the method simpler, faster, more robust, and a useful for hit-to-lead prioritization.

The Rat sarcoma viral oncogene (RAS) family of proteins are GTP/GDP molecular switches and the American Cancer Society estimates that they are mutated in ~19% of all human cancers.(12) The KRas G12D mutation is a highly prevalent oncogenic driver and is frequently found in pancreatic ductal adenocarcinomas (44%) and is associated with low survival rates and high mortality.(13-15) It is also present in around 10-12% of colorectal cancer cases, leading to resistance to anti-EGFR therapy and poor prognosis.(16, 17) KRas G12D is less frequent in non-small cell lung cancer (4%), but it is linked to immunosuppression and resistance to immune checkpoint inhibitors.(18-20) The high prevalence and poor prognosis associated with KRas G12D mutations in various cancers make it an attractive therapeutic target. In recent breakthrough studies from Mirati Therapeutics, MRTX1133 was found to be a potent KRas G12D inhibitor that binds KRas G12D-GDP in a dynamic switch II binding pocket with picomolar affinity.(11) This inhibitor has entered Phase I/II clinical trials.(21) Several compounds belonging to the Mirati MRTX1133 scaffold which bind KRas G12D with a range of affinities have also been found (US Patents WO2021041671, WO2022031678, WO2022132200). Given the importance of KRas G12D in cancer, and the availability of well-characterized chemical matter for this target, we assessed the potential of using LiP-MS in proof-of-concept experiments for KRas G12D protein. We used intact protein mass spectrometry to detect the KRas cleavage products and top-down analysis to identify them, thus locating the cleavage sites in the protein sequence. The inhibitor binding stabilized the protein structure near sites of proteolysis, reducing the degree of cleavage. The extent of the proteolysis reaction was measured quantitatively using intact protein mass spectrometry and was found to be dependent on the drug binding affinity and certain functional groups in the drug's structure. To complement the results obtained by LiP-MS, we conducted molecular dynamics simulations along with

molecular docking to provide atomistic insights into the protein-ligand interactions, and the mechanism of ligand-induced local protein stability. The combination of proteomics techniques and molecular dynamics simulations has previously been used to study a number of biological questions such as protein structure determination,(22) metal-binding events,(23) and lipid-protein interactions.(24) To our knowledge, however, this study represents the first integration of LiP-MS and molecular dynamics to investigate the effects of drug binding on protein dynamics. Our results showed that this approach could be used for the identification of the drug binding sites, for determining critical protein-ligand interactions, and potentially for the secondary screening of drug candidate libraries.

2. Material and Methods

2.1 Protein and drug compounds samples

Recombinant KRas C118S G12D (residues 1-169) protein was expressed in *E.coli* BL21 (DE3) RIL cells using a pET28a vector and purified to homogeneity using standard nickel affinity and size exclusion chromatography. The C118S mutation has no effect on KRas G12D structure but enhances the stability of Ras proteins. The 10 mM DMSO stock solutions of drug compounds used in this study were stored at -20°C until use.

2.2 Proteolytic enzymes and limited proteolysis reactions

For the limited proteolysis reactions, we used two proteolytic enzymes: chymotrypsin (TLCK treated, cat.# LS001432, Worthington) and proteinase K (recombinant, PCR grade, Roche Diagnostics GmbH). All the following solutions were made on the same day of the experiment: the stock solution of the Proteinase K was prepared in 50 mM acetic acid to a final concentration of 0.25 mg/mL. The chymotrypsin stock solution was prepared in LC-MS grade water to give a final concentration of 0.1 mg/mL. The KRas C118S G12D stock solution was diluted in PBS (pH 7.4) to give a final concentration of 10 µM. The drug solutions were each diluted in DMSO to the final concentration of 1 mM. Ten-µL aliquots of the KRas C118S G12D protein solution (final concentration of 10 µM) were incubated in Eppendorf tubes, with 1 µL of each of the drug solutions (final concentration of 100 µM, 1:10 protein to drug), separately, at room temperature (23°C) for 1 hour. Three reaction replicates were prepared for each drug compound. Control samples were prepared by incubating 10 µL of the KRas C118S G12D solution with 1 µL of DMSO under the same conditions. The solutions were then transferred to autosampler vial inserts. Each replicate and the control sample were then incubated sequentially with 1 µL of the proteinase K 0.25 mg/mL at room temperature (23°C) for 5 minutes and subjected to LC-MS analysis. The same number of replicates was used and the same procedures were performed using 0.1 mg/mL chymotrypsin as the proteolytic enzyme solution.

2.3 SDS-PAGE

For SDS-PAGE analysis, the KRas C118S G12D stock solution was diluted in PBS to give a final concentration of 10 μM, and 30 μL of this solution was incubated with 3 μL of the 55085 drug solution (final concentration of 100 μM, 1:10 protein to drug) in 1.5 mL Eppendorf tubes at room temperature (23°C) for 1 hour. The control sample was prepared by incubating 30 μL of the KRas C118S G12D solution with 3 μL of DMSO under the same conditions. The samples containing the 55085 drug and the control samples were then incubated with 3 μL of proteinase K (0.25 mg/mL) or chymotrypsin (0.1 mg/mL) at room temperature for 5 minutes. After incubation, the reactions were quenched by the addition of the 10 μL of the LDS sample buffer (Thermo), and the samples were loaded onto a 1 mm thick Bolt™ 4-12% Bis-Tris Plus precast gel (Thermo) for SDS-PAGE analysis, along with molecular weight markers (Bio-Rad). The electrophoresis was performed at 120 V for 30 minutes, and the gel was subsequently fixed in 10% acetic acid/25% ethanol and stained with 0.01% Coomassie Brilliant Blue G-250 in 10% acetic acid/5% ethanol, followed by destaining in 10% acetic acid.

2.4 LC-MS analysis

Ater incubation, the autosampler vial inserts containing the proteolysis reaction products were then transferred to the autosampler and immediately injected for LC-MS analysis. Intact-protein LC-MS analysis was performed using a Shimadzu Nexera UPLC. AdvanceBio RP-mAb C4 column (2.7 μm particle size, 2.1 mm inner diameter × 50 mm length) coupled to a Sciex TripleTOF 6600+ mass spectrometer. The analysis was performed using a binary gradient with mobile phase A being 0.1% aqueous formic acid (FA) and mobile phase B consisting of

acetonitrile containing 0.1% FA (v/v), with a gradient from 0% to 100% B over 3 minutes, 100%B to 0%B in 0.1 min and holding at 0% B for an additional 2.9 minutes at a flow rate of 200 µL/min. The total run time was 6 minutes. Full MS scans were acquired from 100 to 1500 m/z. The data were processed using Analyst 1.7.2 and PeakView 2.2 with Bio Tool Kit software (Sciex).

For top-down analysis, Information Dependent Acquisition was used with an the inclusion list of pre-selected precursor masses. Precursor ions (742.58^{+16} m/z for Proteinase K cleavage product and 608.8^{+20} m/z for chymotrypsin cleavage product) were included for MS/MS analysis at a retention time of 3.6 minutes for 60 seconds, with an intensity threshold of 1 cps. The top 4 most intense precursor ions were isolated and fragmented with Collision-Induced Dissociation (CID) using a collision energy (CE) of 40 V. The masses of the cleavage products were compared with the theoretical masses of all possible peptides of the KRas C118S G12D protein. The detected fragment masses were searched using Protein Prospector website (https://prospector.ucsf.edu/prospector/mshome.htm).

2.5 Quantitative measurements of proteolysis extent with different drug compounds

To quantitatively assess the degree of cleavage among different drug compound samples with varying affinities and structures, the signal intensities of specific precursors at the maxima of the corresponding chromatographic peaks were measured and compared. For proteinase K, the signal intensity of the 699.88^{+17} m/z peak was recorded, while for chymotrypsin, the signal intensity of the 715.99^{+17} m/z peak was measured.

2.6 Structure preparation and docking

All *in-silico* experiments were performed using the G12D mutant of KRas complexed with MRTX-1133 (PDBID: 7RPZ). Prior to docking, the structure of the protein was prepared using Schrödinger Protein preparation tools with default settings: adding and optimizing hydrogen atoms, setting residue ionization and tautomer states with PROPKA at pH 7, removing water molecules more than 3 Å away from the HET atoms, and performing restrained structure minimization with the OPLS4 force field to converge the heavy atoms to an RMSD of 0.3 Å. This provided minor structure optimization to ensure optimal performance of subsequent docking runs. After protein preparation, the Glide receptor grid was generated, with the grid box centered on 6IC ligand. The structures of all or the ligands were prepared using the LigPrep tool in order to sample all possible conformation states during the docking protocol. Docking was then performed for the series of KRas affinity probest prepared in the previous step. The best models were selected based on the Glide SP docking score, with the top-scored pose chosen as the structural model of the complexes. These structures were then used as inputs for downstream molecular dynamics simulations.

2.7 Molecular dynamics (MD) simulations

The models of the protein-ligand complex identified through docking were used as the initial structures for MD simulations using GROMACS software. All ligands (affinity probes and GDP)

were individually prepared in Pymol, and were then parametrized for CHARMM36 force fields using SwissParam and CHARMM-GUI.(25) The unit cell was established as a rhombic dodecahedron with the protein ≥ 1 nm from all edges. The protein structure was solvated using the TIP3P water model and neutralized with sodium and chloride ions. Particle mesh Ewald (PME) was used for long-range electrostatic interactions, with a 10 Å cutoff for non-bonded interactions. The system was initially equilibrated using an NVT ensemble, followed by further equilibration under NPT conditions. GDP and affinity probes were individually restrained during minimization and equilibration. Production runs were conducted using GROMACS 2020.3 on UNC HPC clusters using Nvidia V100 GPUs. Simulations were at a constant pressure and temperature of 1 atm and 270 K for 500 ns in three replicates with identical parameters. All replicates were individually minimized and equilibrated to obtain unique initial velocity distributions.

2.8 MD data analysis

MD trajectories were processed using MDTraj package in Python. Briefly, trajectories were exported from Gromacs after the removal of the periodic boundary condition end-centering of the protein in the simulation cell. All simulations were exported with a timestep of 1 ns for a total of 500 nanoseconds/frames. To ensure system equilibration, the first 50 ns of the simulations were excluded from further analysis based on the root-mean-square deviation (RMSD) of backbone Cα positions. Analysis was then conducted by selecting protein and ligand structures programmatically and all dynamics used the first frame as a reference.(26) Structural visualizations were generated with PyMOL. Protein-ligand interaction fingerprints were obtained using the ProLIF python package to isolate ligand snapshots and determine intermolecular interactions occurring with a timestep of 10 nanoseconds for a total of 50 snapshots.(27)

3. *Results and Discussion*

LiP-MS analysis was used to characterize the binding of KRas G12D protein with five drug compounds of differing structures and binding affinities. Significant protection from proteolysis was observed upon drug binding, with varying degrees of cleavage for different compounds. The results obtained were explained by comparing MD simulations of free and drug-bound protein-ligand complexes, providing an atomic-level description of the conformational changes upon ligand binding. These simulations revealed key intermolecular interactions and local structural fluctuations in the KRas G12D mutant that are likely responsible for the observed proteolytic patterns.

3.1 Detection of protection from proteolysis of KRas G12D upon drug binding

The proteolytic pattern of the KRas G12D protein showed significant changes upon drug binding, as shown by the SDS-PAGE analysis. The gel analysis indicated that drug binding with compound 55085 led to significant protection against enzymatic cleavage by both proteinase K and chymotrypsin (Figure 4). In the drug-free state, KRas G12D bound to GDP was extensively cleaved into smaller peptides, while in the drug-bound state, the protein showed a distinct reduction in cleavage, suggesting stabilization of the protein structure upon ligand binding. The same finding was confirmed by the intact protein mass LC-MS analyses (Figure 5). New protein charge envelopes were observed which corresponded to the cleavage products of the KRas G12D protein by both proteinase K and chymotrypsin.

	1	2	3	4	5	6	7
KRas G12D	+	+	+	+	+	-	-
55085	-	+	-	+	-	-	-
Proteinase K	+	+	-	-	-	+	-
Chymotrypsin	-	-	+	+	-	-	+

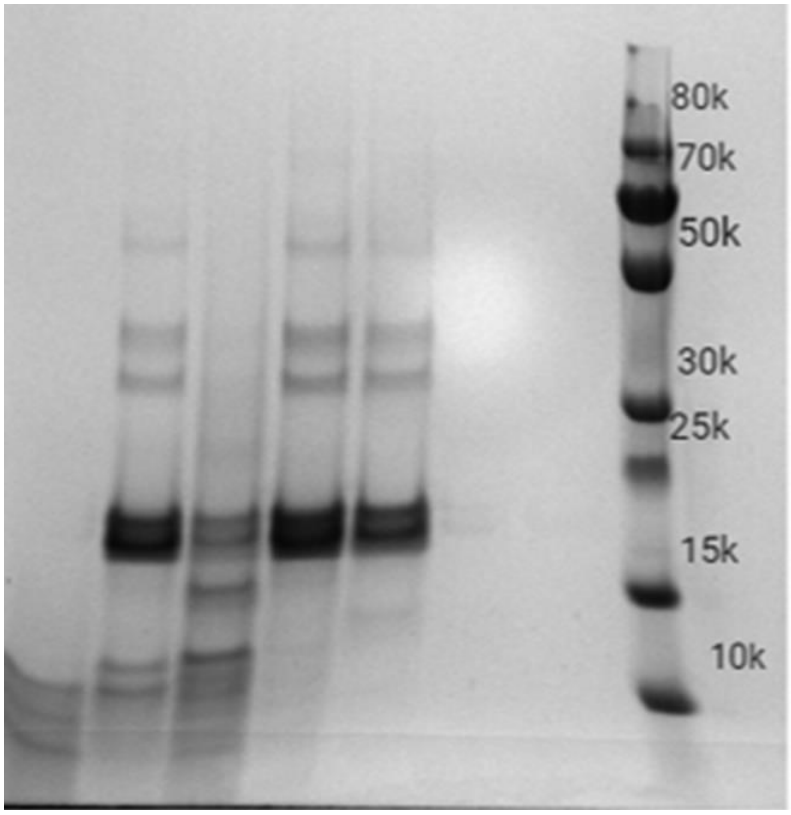

Lane 1 2 3 4 5 6 7 8

Figure 4. SDS-PAGE analysis of limited proteolysis reactions of KRas G12D using two proteolytic enzymes (proteinase K and chymotrypsin) with and without 55085 (MRTX1133). Lane 1, 2 – reaction with proteinase K; lane 3, 4 – reaction with chymotrypsin; lane 5 – intact KRas G12D; lane 6,7 – proteinase K and chymotrypsin controls; lane 8 – molecular weight markers. There is significant protection against the KRas G12D cleavage in the presence of compound 55085.

3.2 Identification of the limited proteolysis cleavage products by LC-MS

The LC-MS analysis of the limited-proteolysis digestion products allowed the precise mapping of the cleavage sites in the KRas G12D protein. In the absence of the drug, the total ion chromatogram revealed distinct peaks corresponding to specific cleavage products. For proteinase K, a cleavage product with a mass of 11,865.4 Da was identified, pinpointing residue M67 as the cleavage site. This was confirmed by top-down analysis with CID fragmentation using a +16 precursor ion at m/z 742.58, which identified the product as the C-terminal portion of the protein (aa68-aa170). Similarly, for chymotrypsin, a cleavage product mass of 12,154.6 Da was identified, corresponding to residue Y64 in the switch-II binding pocket as the cleavage site. CID fragmentation of the +20 precursor ion at m/z 608.8 confirmed this as aa65-aa170 C-terminal part of the protein (Figure 5, 6). The diminished intensities of these specific cleavage products in the drug-bound samples suggests that the binding of the compounds leads to conformational changes that protect this region from proteolysis, indicating the possibility that these residues are located within the drug binding site. Indeed, the drug binding cleavage sites identified by LiP-MS were located at the switch II loop, in agreement with the crystal structure of the KRas G12D+compound 55085 complex (Figure 7).(28)

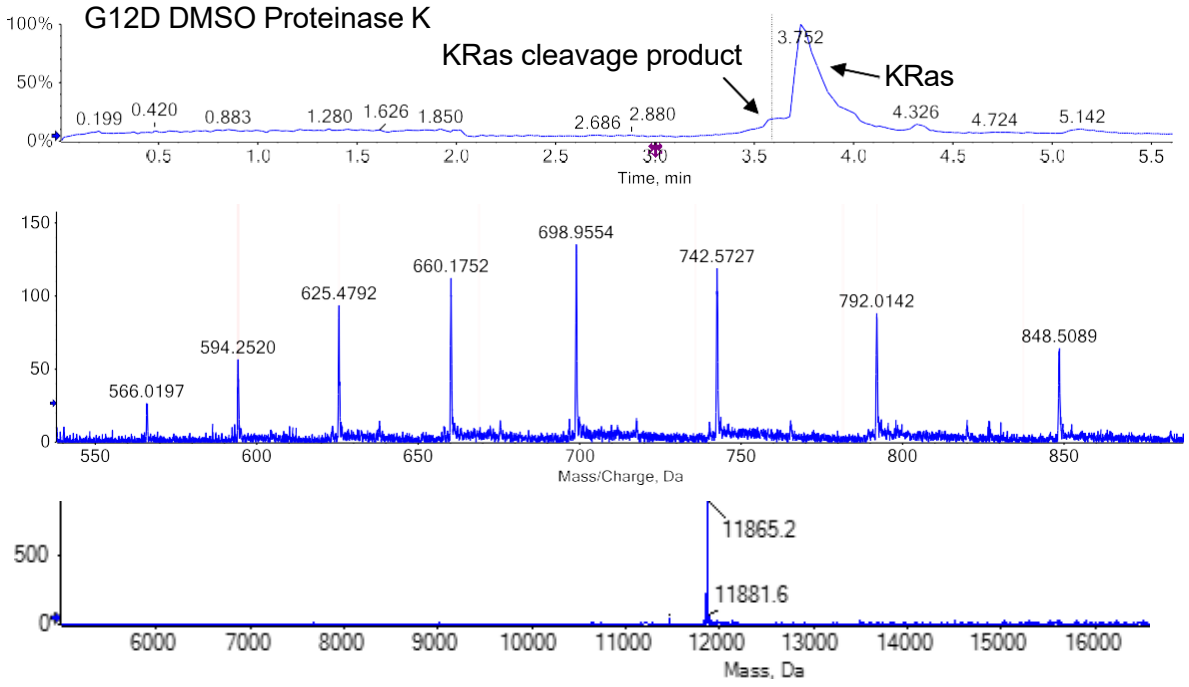
G12D DMSO Proteinase K
KRas cleavage product
KRas
3.752
0.199
0.420
0.883
1.280
1.626
1.850
2.686
2.880
4.326
4.724
5.142
Time, min
698.9554
660.1752
742.5727
625.4792
792.0142
848.5089
594.2520
566.0197
Mass/Charge, Da
11865.2
11881.6
Mass, Da

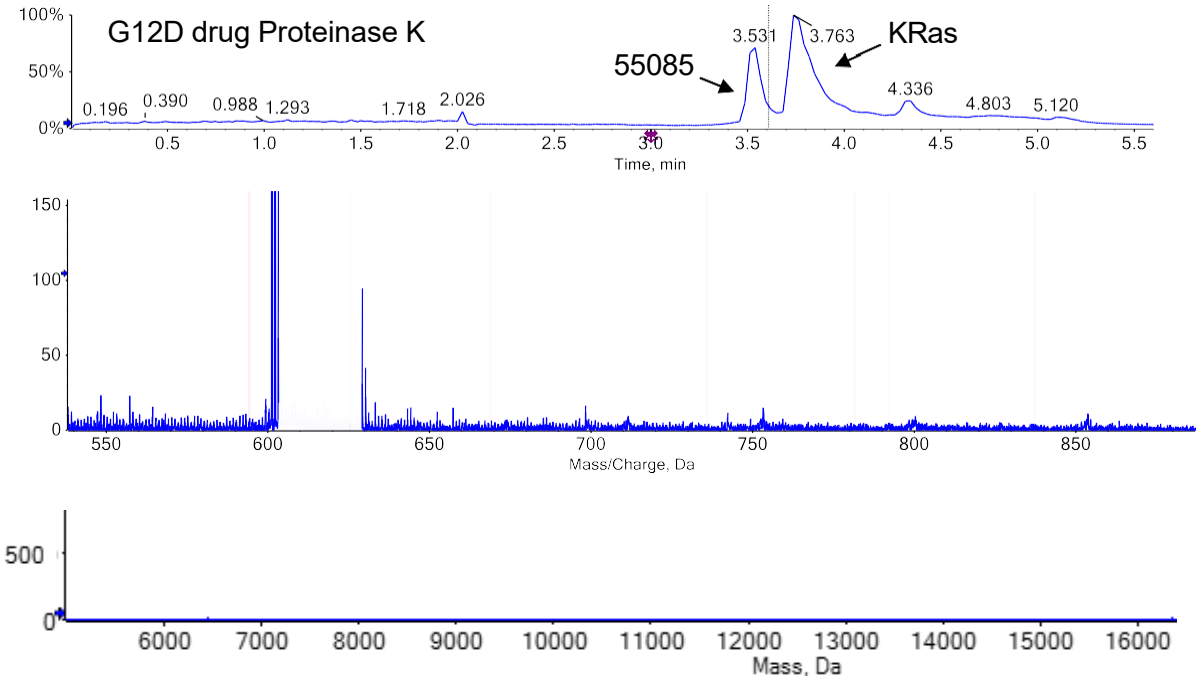
G12D drug Proteinase K
55085
KRas
3.531
3.763
0.196
0.390
0.988
1.293
1.718
2.026
4.336
4.803
5.120
Time, min
Mass/Charge, Da
Mass, Da

KRas cleavage product

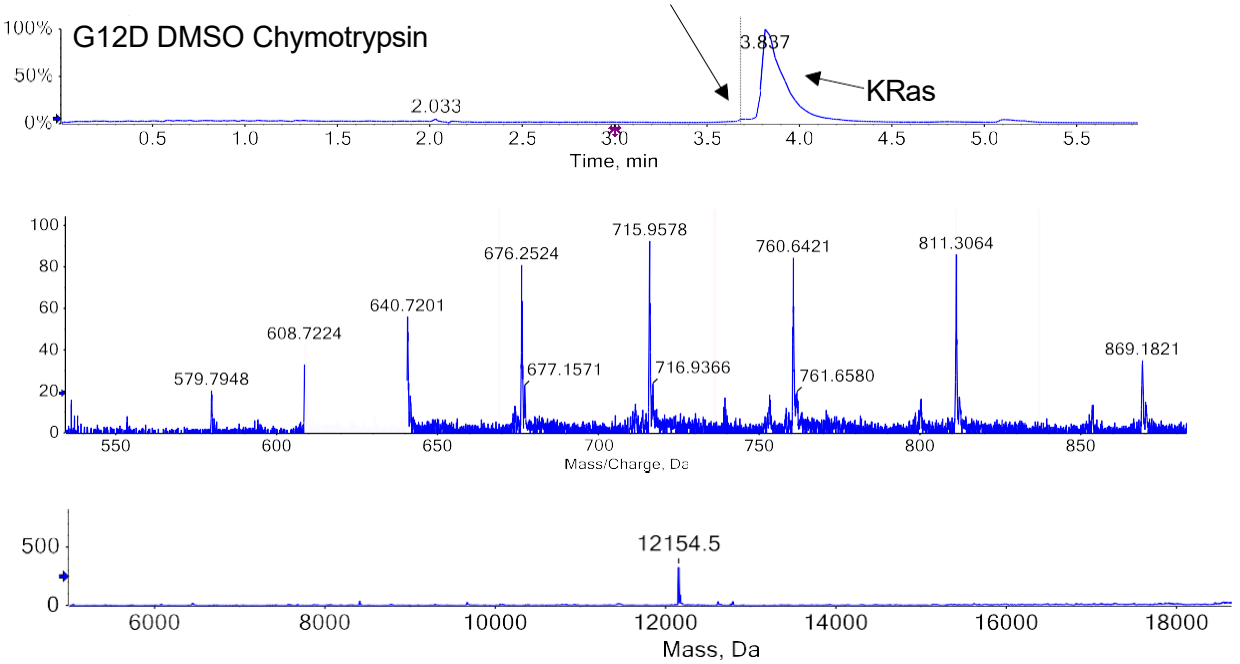

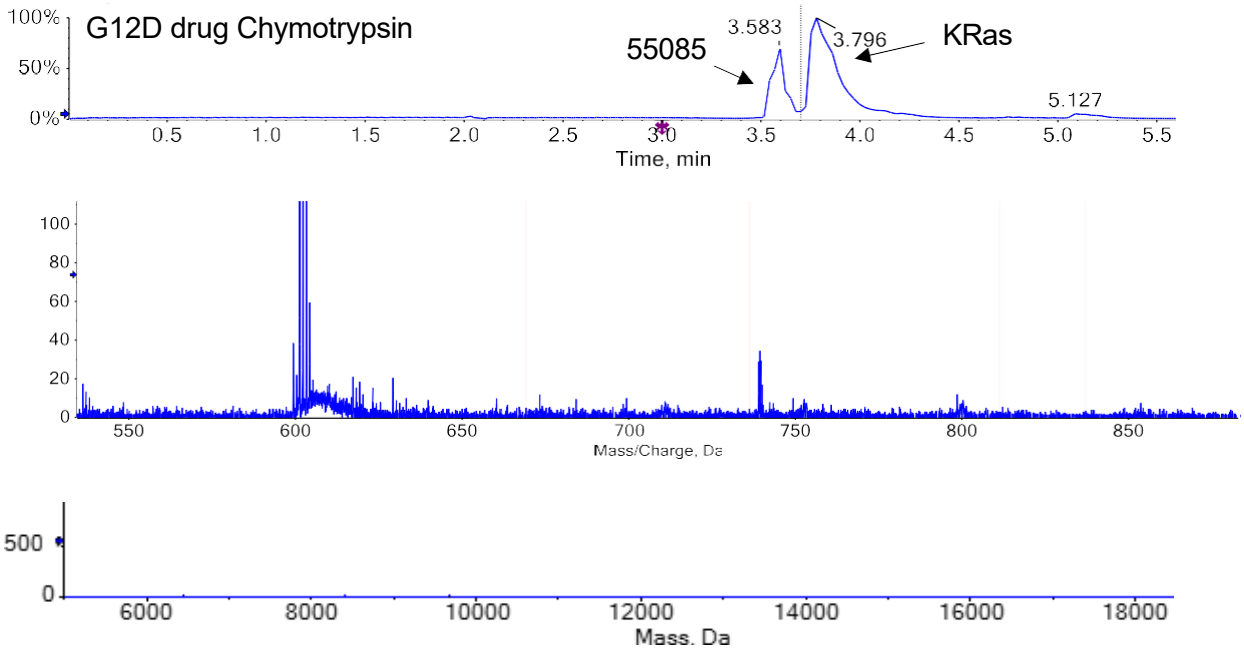

Figure 5. Intact protein LC-MS analysis of KRas G12D limited proteolysis reactions using proteinase K (top) and chymotrypsin (bottom) with and without compound 55085. For each enzyme, the top panel displays spectra without the drug, and the bottom panel displays spectra with the drug. Within each panel, from top to bottom, the data show total ion chromatograms (TICs), representative charge-state envelopes, and the corresponding deconvoluted mass spectra of the protein cleavage products. A noticeable absence of cleavage products is observed in the drug-bound samples.

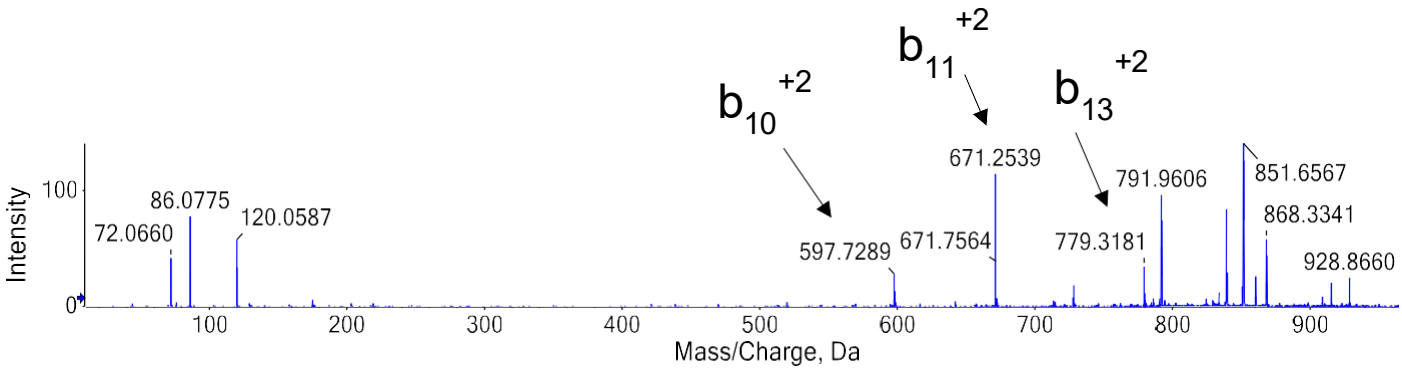

GMTEYKLVVVGADGVGKSALTIQLIQNHFVDEYDPTIEDSYRKQVVIDGETC

LLDILDTAGQEEYSAM$_{67}$RDQYMRTGEGFCVFAINNTKSFEDIHHYREQIKR

VKDSEDVPMVLVGNKSDLPSRTVDTKQAQDLARSYGIPFIETSAKTRQGVD

DAFYTLVREIRKHKEK

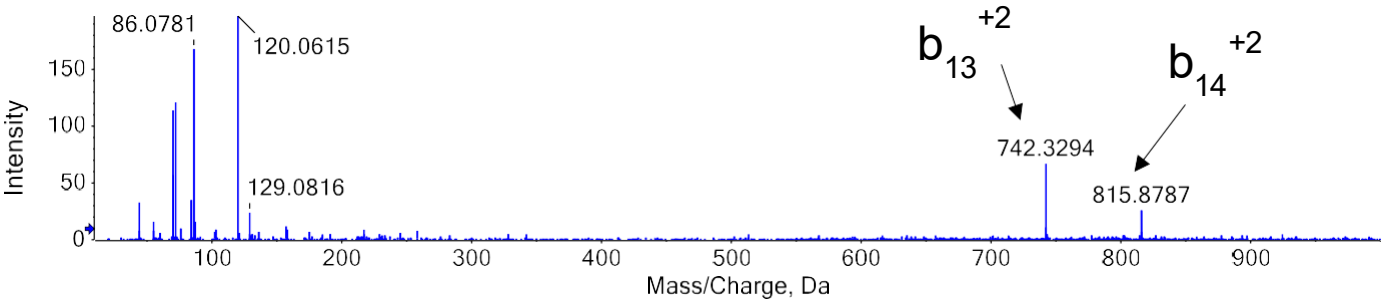

GMTEYKLVVVGADGVGKSALTIQLIQNHFVDEYDPTIEDSYRKQVVIDGETC

LLDILDTAGQEEY$_{64}$SAMRDQYMRTGEGFCVFAINNTKSFEDIHHYREQIKR

VKDSEDVPMVLVGNKSDLPSRTVDTKQAQDLARSYGIPFIETSAKTRQGVD

DAFYTLVREIRKHKEK

Figure 6. Top-down analysis of the KRas G12D cleavage products.

Top, MS/MS mass spectrum of the KRas G12D cleavage product with proteinase K at 11865 Da mass (m/z 742.58^{+16}). Bottom, MS/MS mass spectrum of the KRas G12D cleavage product with chymotrypsin at 12154 Da (m/z 608.08^{+20}). The cleavage products were identified as C-terminal portions of the KRas G12D.

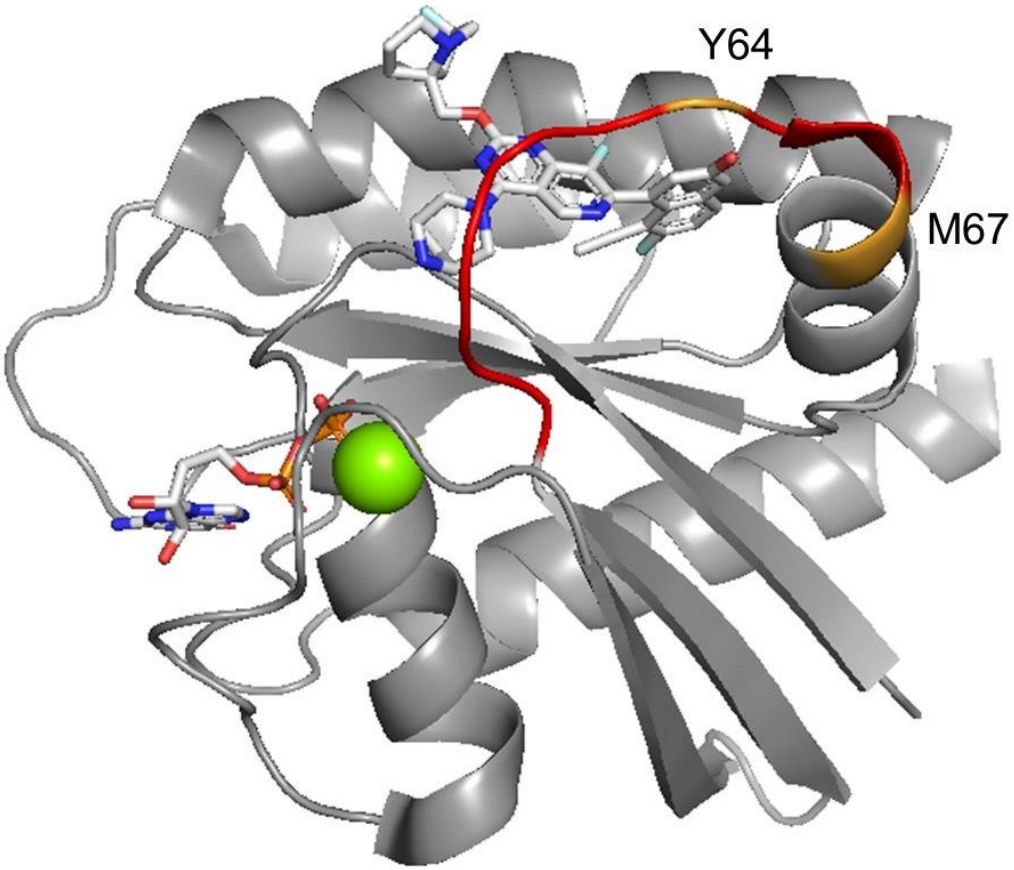

Figure 7. Crystal structure of the KRas G12D – 55085 complex (PDB 7RPZ).

The identified cleavage sites (orange) are located in the switch II loop (red).

3.3 Quantitative analysis of proteolysis extent

The degree of proteolysis was measured quantitatively using the signal intensities of specific precursor ions at the maxima of their chromatographic peaks. For proteinase K, the signal intensity of the 699.88^{+17} m/z precursor was recorded, while for chymotrypsin, the signal intensity of the 715.99^{+17} m/z precursor was measured. The method is robust and rather rapid (~10 minutes per sample). The coefficient of variation (%CV) for the replicates was 7.12% for the proteinase K experiments and 9.97% for the chymotrypsin experiments, indicating high reproducibility of the measurements. Comparisons across different drug compounds with varying affinities revealed differences in the degree of cleavage, correlating with the binding affinities and structural features of the compounds, with the notable exception of compound 54735 (Figure 8). Quantitative measurements of the proteolysis reaction yields, their dependence on the location of the binding site, the binding affinity, and the structure of particular compound makes this method potentially applicable for the screening of drug candidate libraries.

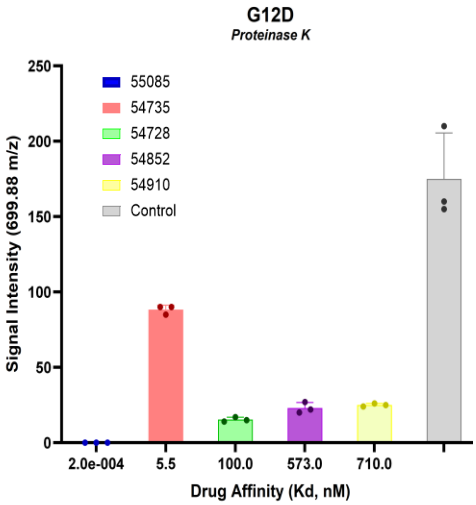
G12D
Proteinase K
Signal Intensity (699.88 m/z)
250
200
150
100
50
0
55085
54735
54728
54852
54910
Control
2.0e-004
5.5
100.0
573.0
710.0
Drug Affinity (Kd, nM)

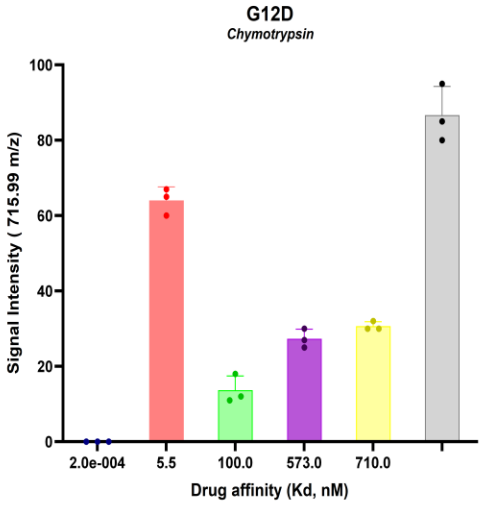
G12D
Chymotrypsin
Signal Intensity (715.99 m/z)
100
80
60
40
20
0
2.0e-004
5.5
100.0
573.0
710.0
Drug affinity (Kd, nM)

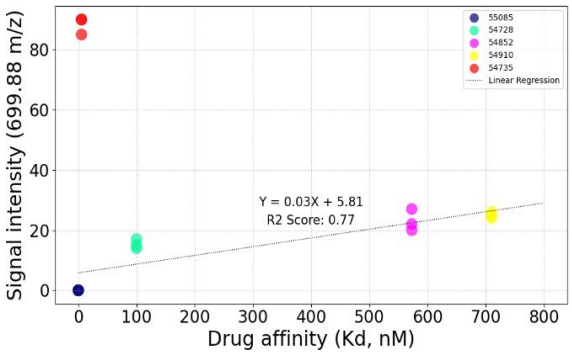
Signal intensity (699.88 m/z)
80
60
40
20
0
0
100
200
300
400
500
600
700
800
Drug affinity (Kd, nM)
55085
54728
54852
54910
54735
Linear Regression
Y = 0.03X + 5.81
R2 Score: 0.77

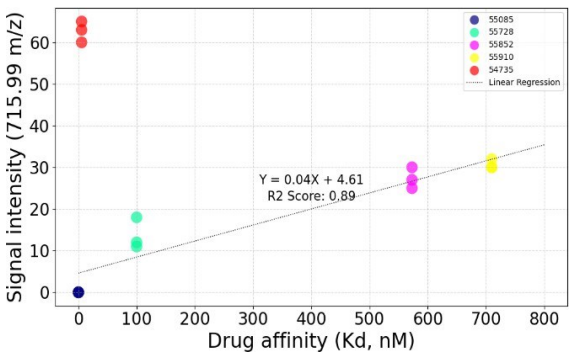
Signal intensity (715.99 m/z)
60
50
40
30
20
10
0
0
100
200
300
400
500
600
700
800
Drug affinity (Kd, nM)
55085
55728
55852
55910
54735
Linear Regression
Y = 0.04X + 4.61
R2 Score: 0.89

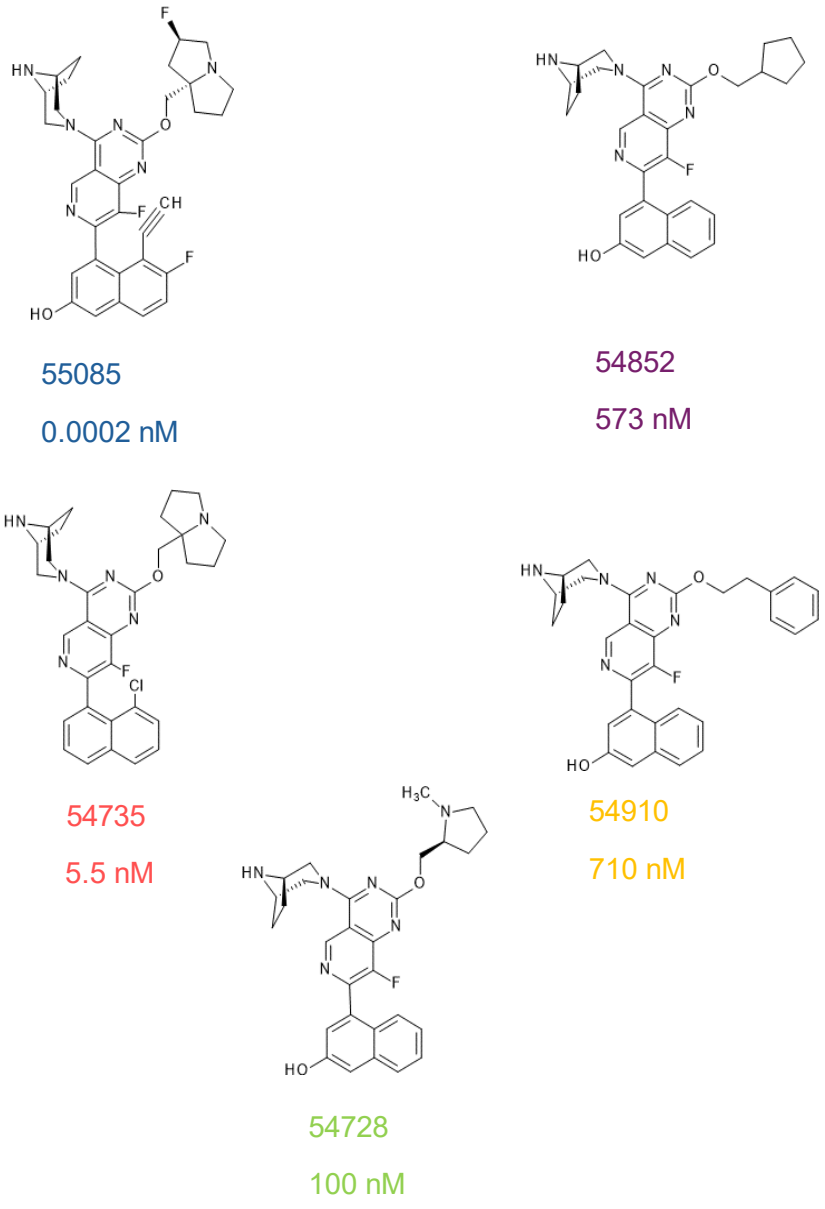

Figure 8.Degree of KRas G12D cleavage depending on compound binding affinities.

Top, degree of cleavage in KRas LiP-MS depending on drug binding affinities. Bottom, structures of compounds used with varying KDs for KRas G12D. There are statistically significant differences in degree of cleavage between the drug-bound and free states of KRas G12D for individual compounds. Notably, there is a correlation of the degree of cleavage in Switch II loop with the KDs of the ligands, with the exception of compound 54735 (Figure S1).

3.4 Characterization of the drug binding by MD simulations

Analysis of the MD trajectories for both the free and drug-bound KRas G12D protein states revealed that ligand binding resulted in a change in flexibility of the LiP-MS cleavage sites located in the switch II region of the protein. We found that the observed root-mean-square fluctuation (RMSF) values, which characterize relative flexibility of the protein along the entire peptide chain, become significantly reduced for the switch II region upon drug binding when compared to the unbound protein complex (Figure 9). Generally, proteases preferentially cleave flexible and locally disordered regions of proteins. The stabilization of the switch II residues observed upon drug binding results in limiting of the movement of the loop away from the core of the protein and, consequently, to a lesser exposure of the cleavage sites to the proteases (Figure 10).

Higher affinity ligands showed greater conformational stability during MD trajectories (Figure 11), retaining more intermolecular interactions within the protein-ligand complex (Figure 12, Figure S2). This led to a more stable switch II region, corroborating the patterns observed in LiP-MS. The mobility of the ligand at the drug binding site modulates the mobility of the switch II loop and, consequently, increases the exposure of the cleavage sites to the proteases. The correlation between the binding affinity and the degree of limited proteolysis can be explained in this way. In addition, the presence or absence of a particular functional group can also affect the extent of limited proteolysis. A detailed analysis of the KRas G12D–54735 ligand simulation explains the deviation in the correlation trend between the binding affinity and the degree of proteolysis observed for the other compounds. The 54735 compound lacks an -OH group, which is present in all the other compounds, and this functional group interacts with D69 side chain.

The lack of stabilizing coordination at D69 results in a higher degree of exposure of the neighboring proteolytic site (Figure S1, Figure S2).

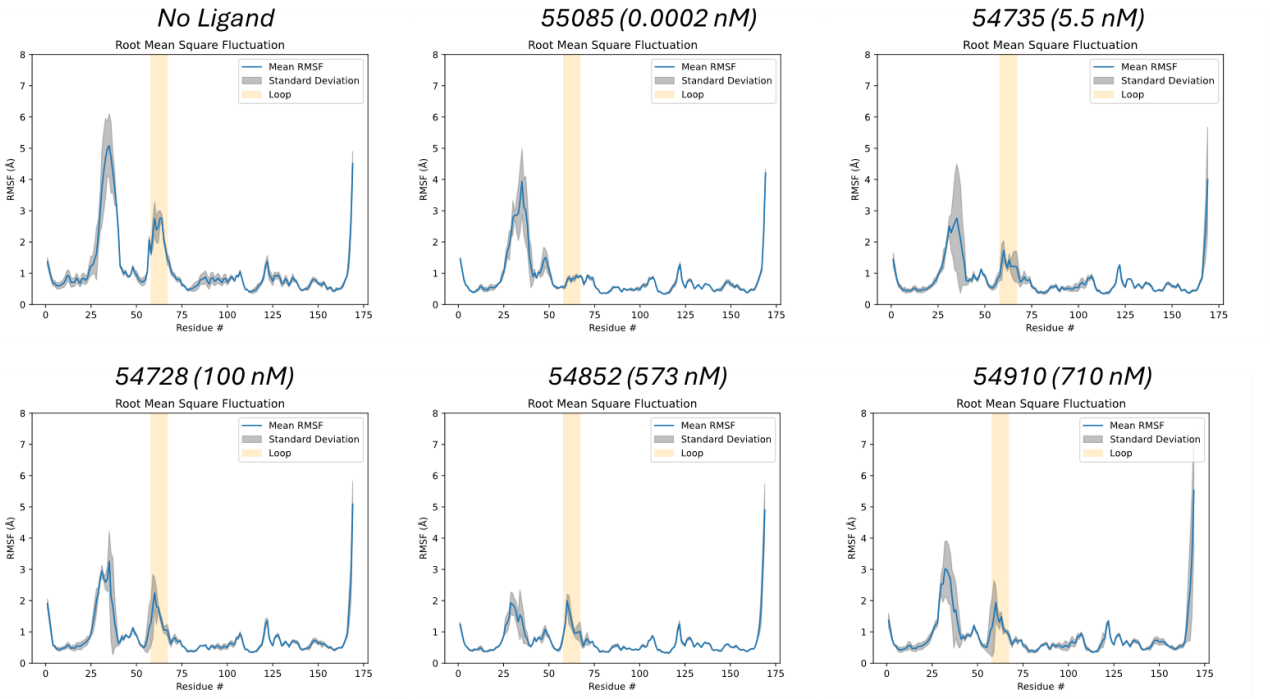

Figure 9. Change in KRas G12D protein fluctuation upon ligand binding characterized by root-mean-squared fluctuation (RMSF).

The average of three replicates is shown, with standard deviation in gray. In general, drug binding limits the mobility of the switch II region (58-67), highlighted in orange. The switch II fluctuations decrease with an increase in the drug binding affinity.

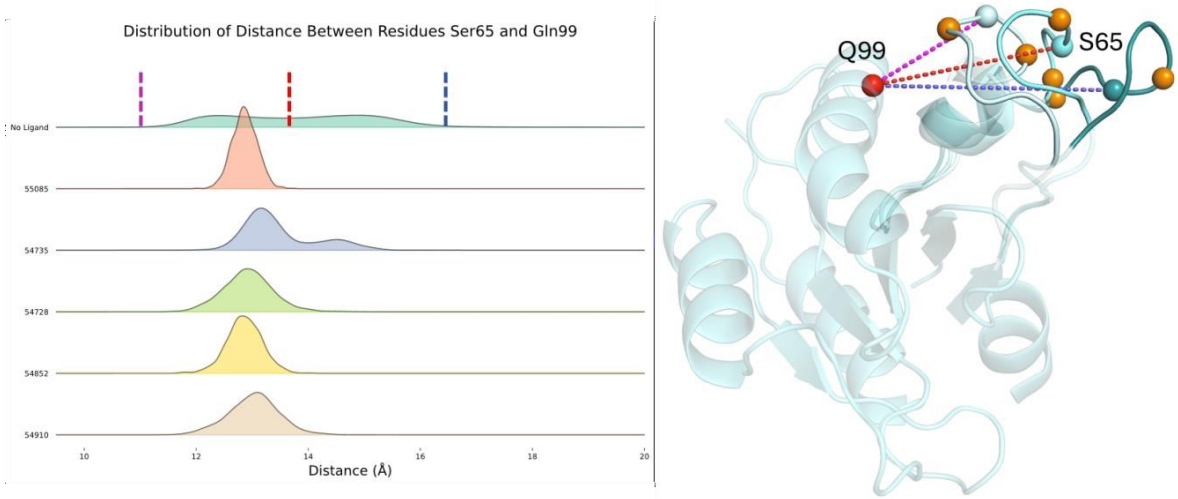

Figure 10. Distribution of distances between residue S65, located between the cleavage sites Y64 and M67 (orange spheres), and the reference residue Q99 on the core of the protein.

The width of a distribution corresponds to the magnitude of distance fluctuations during the simulations. Drug binding stabilizes switch II fluctuations, as evidenced by the reduced width of the distributions, and pulls the loop closer to the rest of the protein, as indicated by the leftward shift of the distributions. Min (magenta), max (purple), and median (orange) distances are displayed as dashed lines on the distributions for unbound KRas. The same distances are shown in the corresponding snapshots from the MD simulation on the unbound KRas structure.

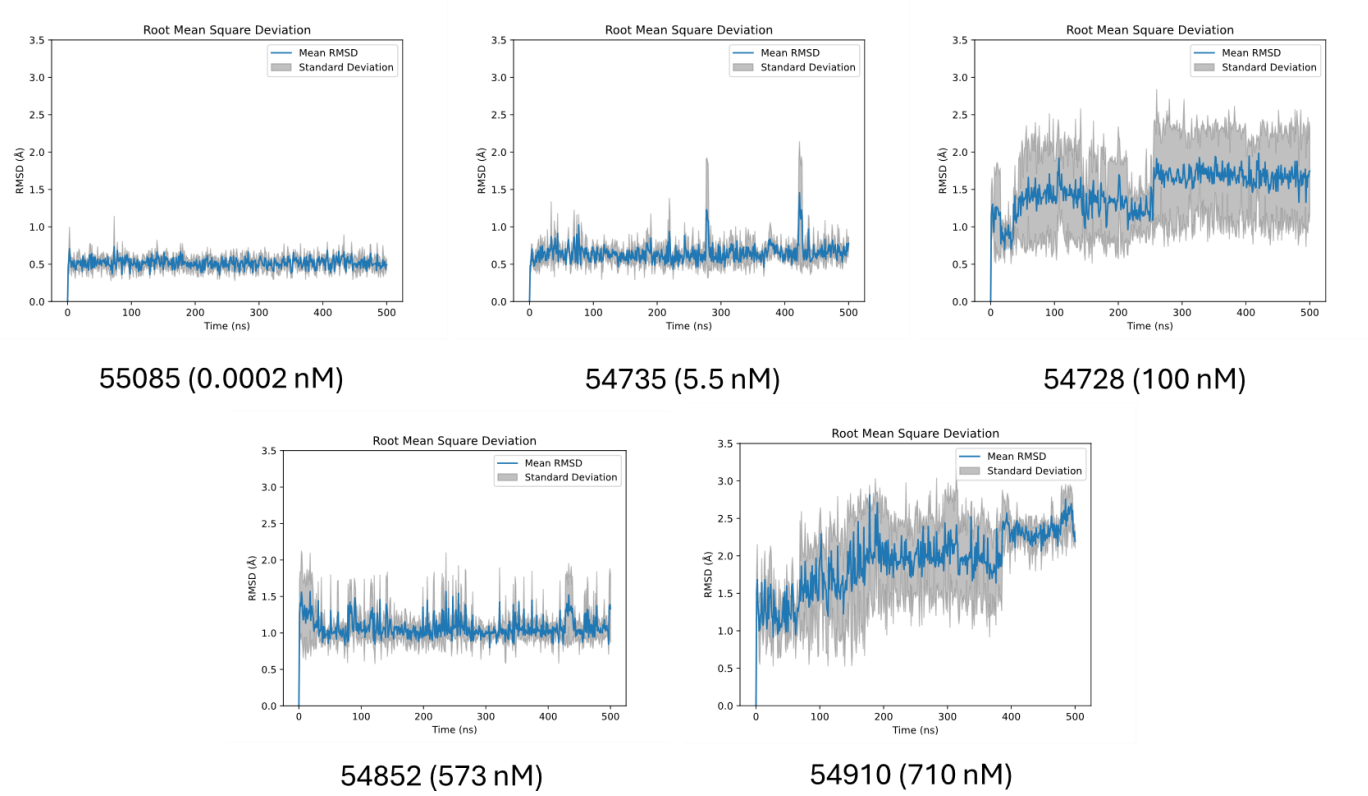

Figure 11. KRas G12D interaction with ligands of differing affinities.

A. Dynamics of ligands bound to the KRas G12D. Lower ligand mobility (lower RMSD) is observed for high-affinity ligands.

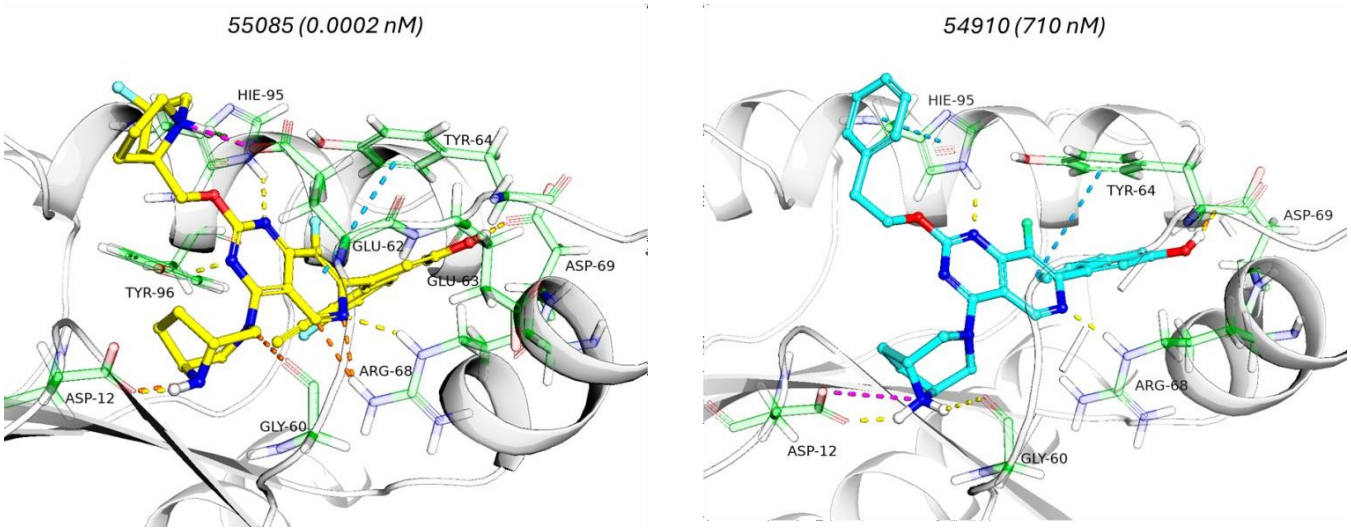

Figure 12. Structural models for the KRas G12D-drug complexes with compounds 55085 and 54910, as identified by molecular docking.

Higher-affinity ligands exhibit a more extended protein-ligand interaction network (Figure S2), including interactions with the switch II region.

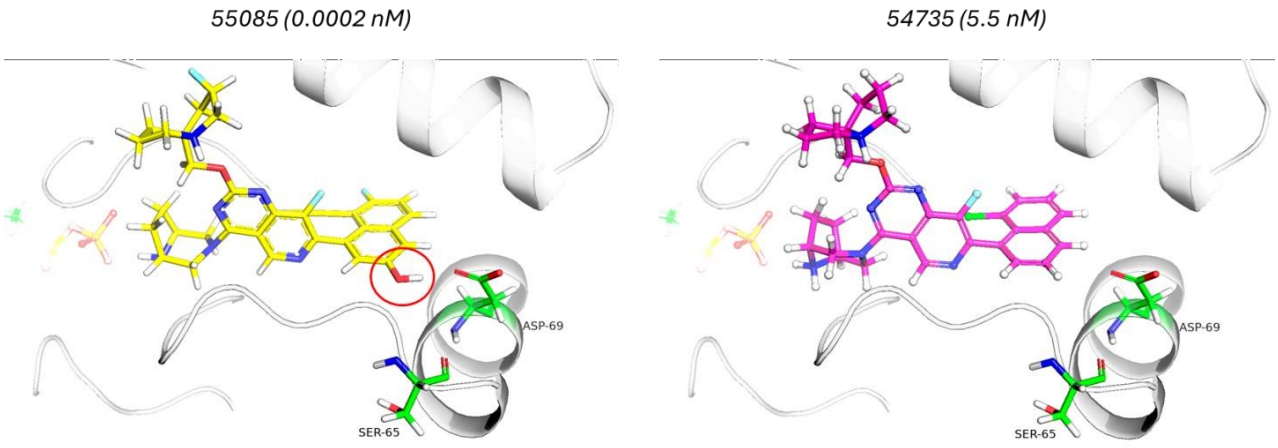

Supplementary Figure 1. Interactions between ligand functional groups and the switch II loop residues.

Docked structures of 55085 and 54735 show interaction of 55085's -OH group (highlighted with a red circle) group with the residue D69. This -OH group and corresponding interactions are absent in the case of 54735. In addition, transient hydrogen bonding also occurs with S65 and the same OH group during the simulation (Figure S2). Lack of these interactions can explain the deviation in the correlation trend between binding affinity and degree of cleavage in the switch II loop for compound 54735.

55085 (0.0002 nM)

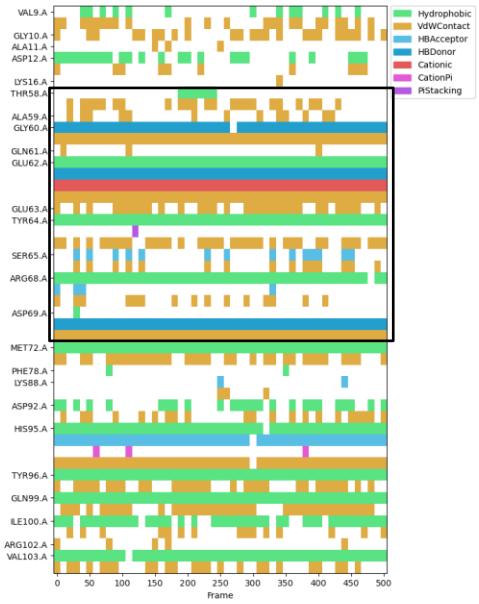

54735 (5.5 nM)

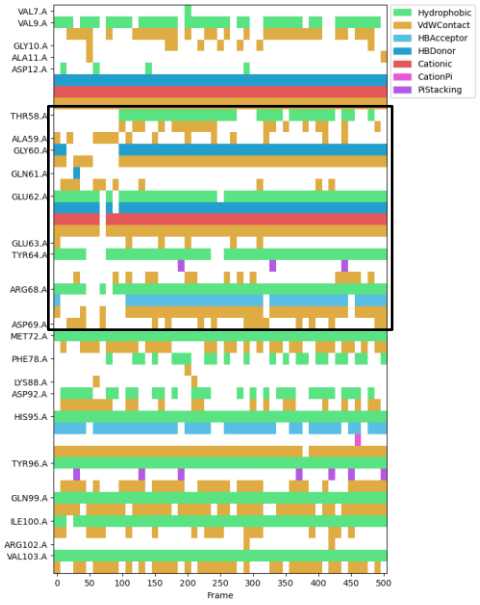

54728 (100 nM)

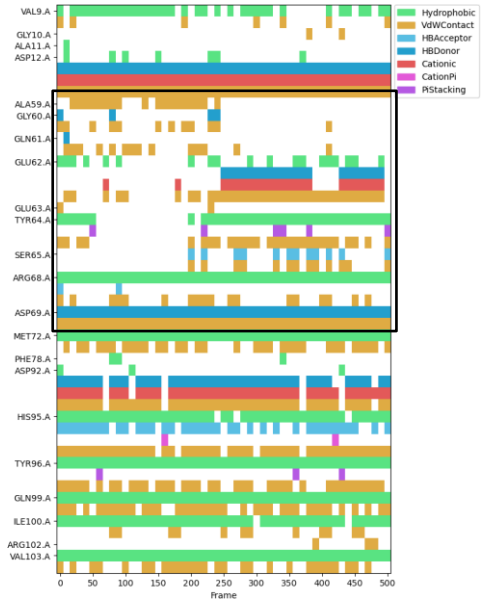

54852 (573 nM)

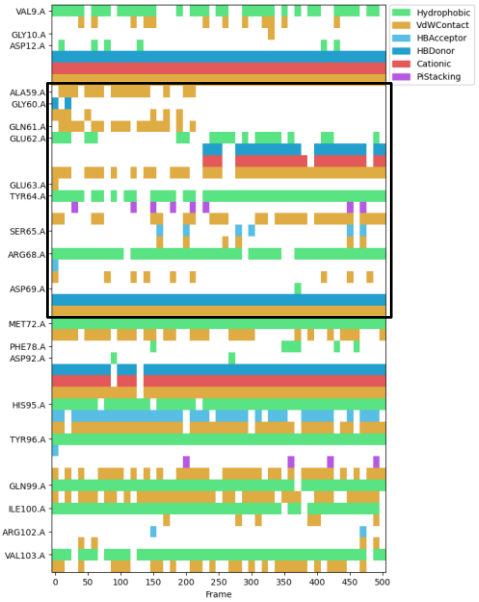

54S10 (710 nM)

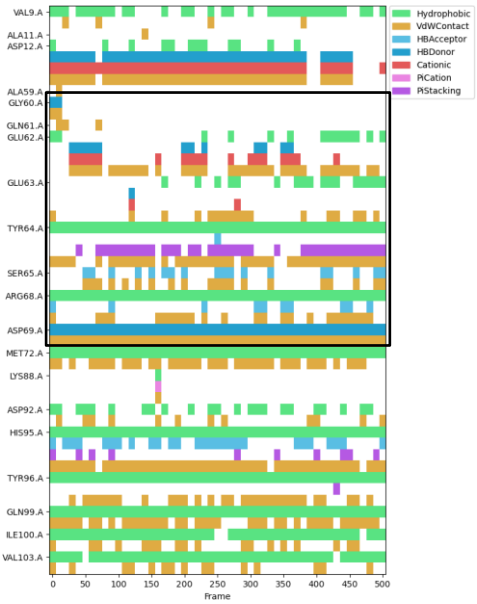

Supplementary Figure 2. Interaction of ligand functional groups with the KRas G12D residues.

Computed KRAS G12D-drug interactions computed over the course of the simulations. The black box highlights the switch II region for each complex. Higher-affinity ligands show a higher number of interactions with a more consistent pattern along the simulation, stabilizing the ligand and the surrounding protein pocket.

4. Conclusion

The combination of LiP-MS and MD analyses for the KRas G12D mutant in complex with various ligands, as shown in this work, enabled the determination of the drug binding site on the protein, the ranking of ligands according to their binding affinities, the characterization of key protein-ligand interactions, and an improved understanding of the structural and proteolysis changes that occur upon ligand binding. These capabilities make these techniques valuable tools in structure-based drug discovery and a powerful addition to traditional methods for screening of small lead compound libraries. LiP-MS coupled with MD simulations represents a novel approach which can be useful for the drug design and development.

References

1. Piazza I, Kochanowski K, Cappelletti V, Fuhrer T, Noor E, Sauer U, et al. A Map of Protein-Metabolite Interactions Reveals Principles of Chemical Communication. Cell. 2018;172(1-2):358-72 e23.

2. Piazza I, Beaton N, Bruderer R, Knobloch T, Barbisan C, Chandat L, et al. A machine learning-based chemoproteomic approach to identify drug targets and binding sites in complex proteomes. Nat Commun. 2020;11(1):4200.

3. Cappelletti V, Hauser T, Piazza I, Pepelnjak M, Malinovska L, Fuhrer T, et al. Dynamic 3D proteomes reveal protein functional alterations at high resolution in situ. Cell. 2021;184(2):545-59 e22.

4. Petrotchenko EV, Nascimento EM, Witt JM, Borchers CH. Determination of Protein Monoclonal-Antibody Epitopes by a Combination of Structural Proteomics Methods. J Proteome Res. 2023;22(9):3096-102.

5. Serpa JJ, Popov KI, Petrotchenko EV, Dokholyan NV, Borchers CH. Structure of prion beta-oligomers as determined by short-distance crosslinking constraint-guided discrete molecular dynamics simulations. Proteomics. 2021;21(21-22):e2000298.

6. Holfeld A, Quast JP, Bruderer R, Reiter L, de Souza N, Picotti P. Limited Proteolysis-Mass Spectrometry to Identify Metabolite-Protein Interactions. Methods Mol Biol. 2023;2554:69-89.

7. Schopper S, Kahraman A, Leuenberger P, Feng Y, Piazza I, Muller O, et al. Measuring protein structural changes on a proteome-wide scale using limited proteolysis-coupled mass spectrometry. Nat Protoc. 2017;12(11):2391-410.

8. Feng Y, De Franceschi G, Kahraman A, Soste M, Melnik A, Boersema PJ, et al. Global analysis of protein structural changes in complex proteomes. Nat Biotechnol. 2014;32(10):1036-44.

9. Mackmull MT, Nagel L, Sesterhenn F, Muntel J, Grossbach J, Stalder P, et al. Global, in situ analysis of the structural proteome in individuals with Parkinson's disease to identify a new class of biomarker. Nat Struct Mol Biol. 2022;29(10):978-89.

10. Reber V, Gstaiger M. Target Deconvolution by Limited Proteolysis Coupled to Mass Spectrometry. Methods Mol Biol. 2023;2706:177-90.

11. Wang X, Allen S, Blake JF, Bowcut V, Briere DM, Calinisan A, et al. Identification of MRTX1133, a Noncovalent, Potent, and Selective KRAS(G12D) Inhibitor. J Med Chem. 2022;65(4):3123-33.

12. Jedrzejewski PT, Lehmann WD. Detection of modified peptides in enzymatic digests by capillary liquid chromatography/electrospray mass spectrometry and a progammable skimmer CID acquisition routine. Anal Chem. 1997;69:294-301.

13. Sung H, Ferlay J, Siegel RL, Laversanne M, Soerjomataram I, Jemal A, et al. Global Cancer Statistics 2020: GLOBOCAN Estimates of Incidence and Mortality Worldwide for 36 Cancers in 185 Countries. CA Cancer J Clin. 2021;71(3):209-49.

14. Stickler S, Rath B, Hamilton G. Targeting KRAS in pancreatic cancer. Oncol Res. 2024;32(5):799-805.

15. Bournet B, Muscari F, Buscail C, Assenat E, Barthet M, Hammel P, et al. KRAS G12D Mutation Subtype Is A Prognostic Factor for Advanced Pancreatic Adenocarcinoma. Clin Transl Gastroenterol. 2016;7(3):e157.

16. Feng J, Hu Z, Xia X, Liu X, Lian Z, Wang H, et al. Feedback activation of EGFR/wild-type RAS signaling axis limits KRAS(G12D) inhibitor efficacy in KRAS(G12D)-mutated colorectal cancer. Oncogene. 2023;42(20):1620-33.

17. Lievre A, Bachet JB, Le Corre D, Boige V, Landi B, Emile JF, et al. KRAS mutation status is predictive of response to cetuximab therapy in colorectal cancer. Cancer Res. 2006;66(8):3992-5.

18. Zeissig MN, Ashwood LM, Kondrashova O, Sutherland KD. Next batter up! Targeting cancers with KRAS-G12D mutations. Trends Cancer. 2023;9(11):955-67.

19. Van de Water J, Deininger SO, Macht M, Przybylski M, Gershwin ME. Detection of molecular determinants and epitope mapping using MALDI-TOF mass spectrometry. Clin Immun Immunpath. 1997;85:229-35.

20. Liu C, Zheng S, Wang Z, Wang S, Wang X, Yang L, et al. KRAS-G12D mutation drives immune suppression and the primary resistance of anti-PD-1/PD-L1 immunotherapy in non-small cell lung cancer. Cancer Commun (Lond). 2022;42(9):828-47.

21. Kakimoto T. CKI1, a histidine kinase homolog implicated in cytokinin signal transduction. Science. 1996;274:982-5.

22. Marklund EG, Benesch JL. Weighing-up protein dynamics: the combination of native mass spectrometry and molecular dynamics simulations. Curr Opin Struct Biol. 2019;54:50-8.

23. Peris-Diaz MD, Guran R, Domene C, de Los Rios V, Zitka O, Adam V, et al. An Integrated Mass Spectrometry and Molecular Dynamics Simulations Approach Reveals the Spatial Organization Impact of Metal-Binding Sites on the Stability of Metal-Depleted Metallothionein-2 Species. J Am Chem Soc. 2021;143(40):16486-501.

24. Costeira-Paulo J, Gault J, Popova G, Ladds M, van Leeuwen IMM, Sarr M, et al. Lipids Shape the Electron Acceptor-Binding Site of the Peripheral Membrane Protein Dihydroorotate Dehydrogenase. Cell Chem Biol. 2018;25(3):309-17 e4.

25. Jo S, Kim T, Iyer VG, Im W. CHARMM-GUI: a web-based graphical user interface for CHARMM. J Comput Chem. 2008;29(11):1859-65.

26. McGibbon RT, Beauchamp KA, Harrigan MP, Klein C, Swails JM, Hernandez CX, et al. MDTraj: A Modern Open Library for the Analysis of Molecular Dynamics Trajectories. Biophys J. 2015;109(8):1528-32.

27. Bouysset C, Fiorucci S. ProLIF: a library to encode molecular interactions as fingerprints. J Cheminform. 2021;13(1):72.

28. Gunn RJ, Thomas, N.C., Xiaolun, W., Lawson, J.D., Marx, M.A. KRAS G12D in complex with MRTX-1133 2021-12-22 [https://www.rcsb.org/structure/7RPZ].

Chapter 3: Final Conclusion and General Discussion

The findings presented in this thesis have provided significant insights into the application of Limited Proteolysis-Mass Spectrometry (LiP-MS) combined with Molecular Dynamics (MD) simulations to characterize interactions between small molecules and the KRas G12D mutant oncoprotein. By combining both experimental and computational approaches, this work has led to a comprehensive understanding of the structural changes that happen upon drug binding, therefore contributing critical data to drug discovery efforts targeting KRas.

A key achievement of this research was demonstrating that LiP-MS can map protein-ligand interactions at high resolution. The data revealed KRas G12D protection from proteolysis at specific sites upon ligand binding, indicating the stabilization of flexible protein regions. This finding was supported by MD simulations. It showed decreased fluctuation of key residues, reinforcing the hypothesis that the drug molecules stabilize specific protein regions and potentially inhibit oncogenic signaling.

Quantitative proteolysis analysis further underscored the utility of LiP-MS for ranking ligands based on their binding affinities, correlating proteolysis yields with compound affinities, and establishing it as a promising tool for rapid candidate prioritization in drug discovery. The methodology's adaptability extends beyond KRas G12D, offering potential applications for other proteins in cancer and various diseases. Combining LiP-MS with MD simulations demonstrated a deeper mechanistic understanding of drug-protein interactions, enhancing early-stage drug discovery and hit-to-lead optimization.

However, limitations must be noted. Not all proteins are readily detectable by MS, and some may not undergo significant structural changes upon ligand binding, limiting the method's general applicability. Furthermore, during initial cleavage reactions, incomplete detection of the second half of the protein introduced some ambiguity. These challenges suggest further refinement, such as optimizing proteolysis reactions for clearer single cleavage patterns.

A comparison of the findings with other MD simulation studies (72-74) reveals both consistency and unique contributions. For instance, the observed stabilization of the switch II region upon ligand binding in this study aligns with the findings of Issahaku et al. , which also highlighted the critical role of switch regions in KRas stability.(72) Similarly, the study of Tu et al. emphasized the significance of functional groups in ligand interactions, consistent with the role of the hydroxyl group identified in this study.(73) However, this work uniquely integrates LiP-MS data with MD simulations to provide an experimental validation of structural stabilization, which is absent in these comparative studies. Such integration offers complementary insights, bridging computational predictions and experimental evidence.

Future work should aim to enhance the sensitivity of LiP-MS for proteins less compatible with LC-MS techniques, potentially using different proteases or adjusting LC-MS protocols. Expanding the method to lower-affinity compounds could help define the threshold at which binding effects remain detectable, refining the technique for broader applications. Incorporating complementary structural proteomics techniques like hydrogen-deuterium exchange (HDX), cross-linking, and surface modification can provide additional layers of structural insight. HDX assesses hydrogen bonding and secondary structure by measuring exchange rates, while cross-linking preserves spatial constraints, and surface modification identifies exposed regions on the protein. Integrating these techniques with computational approaches like MD simulations enriches the understanding

of small molecule-protein interactions, as demonstrated in this study.

Applying this methodology to other disease-related proteins and drug-resistant mutations could further enhance its value in drug discovery. By extending LiP-MS to such targets, new therapeutic avenues may be uncovered, and lead compounds more effectively optimized.

In conclusion, this thesis has underscored the effectiveness of the integrated LiP-MS-MD approach for investigating protein-drug interactions. The combination of experimental and computational data provided a comprehensive view of protein dynamics and interaction sites. This work enabled the determination of drug binding sites, ranking of ligands based on binding affinities, and detailed characterization of key interactions, offering a powerful tool for drug discovery. LiP-MS coupled with MD simulations complements traditional screening methods and presents a promising strategy for drug design and development, with potential applications across a wide range of proteins and therapeutic areas.

References

1. Beck H, Harter M, Hass B, Schmeck C, Baerfacker L. Small molecules and their impact in drug discovery: A perspective on the occasion of the 125th anniversary of the Bayer Chemical Research Laboratory. Drug Discov Today. 2022;27(6):1560-74.

2. Blay V, Tolani B, Ho SP, Arkin MR. High-Throughput Screening: today's biochemical and cell-based approaches. Drug Discov Today. 2020;25(10):1807-21.

3. Fang Y. Ligand-receptor interaction platforms and their applications for drug discovery. Expert Opin Drug Discov. 2012;7(10):969-88.

4. Stoddart LA, White CW, Nguyen K, Hill SJ, Pfleger KD. Fluorescence- and bioluminescence-based approaches to study GPCR ligand binding. Br J Pharmacol. 2016;173(20):3028-37.

5. Bergsdorf C, Ottl J. Affinity-based screening techniques: their impact and benefit to increase the number of high quality leads. Expert Opin Drug Discov. 2010;5(11):1095-107.

6. Coussens NP, Auld DS, Thielman JR, Wagner BK, Dahlin JL. Addressing Compound Reactivity and Aggregation Assay Interferences: Case Studies of Biochemical High-Throughput Screening Campaigns Benefiting from the National Institutes of Health Assay Guidance Manual Guidelines. SLAS Discov. 2021;26(10):1280-90.

7. Dahlin JL, Nissink JW, Strasser JM, Francis S, Higgins L, Zhou H, et al. PAINS in the assay: chemical mechanisms of assay interference and promiscuous enzymatic inhibition observed during a sulfhydryl-scavenging HTS. J Med Chem. 2015;58(5):2091-113.

8. Fontana A, de Laureto PP, Spolaore B, Frare E, Picotti P, Zambonin M. Probing protein structure by limited proteolysis. Acta Biochim Pol. 2004;51(2):299-321.

9. Schopper S, Kahraman A, Leuenberger P, Feng Y, Piazza I, Muller O, et al. Measuring protein structural changes on a proteome-wide scale using limited proteolysis-coupled mass spectrometry. Nat Protoc. 2017;12(11):2391-410.

10. Feng Y, De Franceschi G, Kahraman A, Soste M, Melnik A, Boersema PJ, et al. Global analysis of protein structural changes in complex proteomes. Nat Biotechnol. 2014;32(10):1036-44.

11. Leuenberger P, Ganscha S, Kahraman A, Cappelletti V, Boersema PJ, von Mering C, et al. Cell-wide analysis of protein thermal unfolding reveals determinants of thermostability. Science. 2017;355(6327).

12. Picotti P, Marabotti A, Negro A, Musi V, Spolaore B, Zambonin M, et al. Modulation of the structural integrity of helix F in apomyoglobin by single amino acid replacements. Protein Sci. 2004;13(6):1572-85.

13. Martini F, Aceto A, Sacchetta P, Bucciarelli T, Dragani B, Di Ilio C. Investigation of intra-domain and inter-domain interactions of glutathione transferase P1-1 by limited chymotryptic cleavage. Eur J Biochem. 1993;218(3):845-51.

14. Fontana A, de Laureto PP, Spolaore B, Frare E. Identifying disordered regions in proteins by limited proteolysis. Methods Mol Biol. 2012;896:297-318.

15. Wang L, Chen RX, Kallenbach NR. Proteolysis as a probe of thermal unfolding of cytochrome c. Proteins. 1998;30(4):435-41.

16. Park C, Marqusee S. Probing the high energy states in proteins by proteolysis. J Mol Biol. 2004;343(5):1467-76.

17. Acquasaliente L, Pelc LA, Di Cera E. Probing prothrombin structure by limited proteolysis. Sci Rep. 2019;9(1):6125.

18. Shevchenko A, Tomas H, Havlis J, Olsen JV, Mann M. In-gel digestion for mass spectrometric characterization of proteins and proteomes. Nat Protoc. 2006;1(6):2856-60.

19. Serpa JJ, Patterson AP, Pan J, Han J, Wishart DS, Petrotchenko EV, et al. Using multiple structural proteomics approaches for the characterization of prion proteins. J Proteomics. 2013;81:31-42.

20. Breuker K, Jin M, Han X, Jiang H, McLafferty FW. Top-down identification and characterization of biomolecules by mass spectrometry. J Am Soc Mass Spectrom. 2008;19(8):1045-53.

21. Cappelletti V, Hauser T, Piazza I, Pepelnjak M, Malinovska L, Fuhrer T, et al. Dynamic 3D proteomes reveal protein functional alterations at high resolution in situ. Cell. 2021;184(2):545-59 e22.

22. Piazza I, Beaton N, Bruderer R, Knobloch T, Barbisan C, Chandat L, et al. A machine learning-based chemoproteomic approach to identify drug targets and binding sites in complex proteomes. Nat Commun. 2020;11(1):4200.

23. Petrotchenko EV, Nascimento EM, Witt JM, Borchers CH. Determination of Protein Monoclonal-Antibody Epitopes by a Combination of Structural Proteomics Methods. J Proteome Res. 2023;22(9):3096-102.

24. Serpa JJ, Popov KI, Petrotchenko EV, Dokholyan NV, Borchers CH. Structure of prion beta-oligomers as determined by short-distance crosslinking constraint-guided discrete molecular dynamics simulations. Proteomics. 2021;21(21-22):e2000298.

25. Piazza I, Kochanowski K, Cappelletti V, Fuhrer T, Noor E, Sauer U, et al. A Map of Protein-Metabolite Interactions Reveals Principles of Chemical Communication. Cell. 2018;172(1-2):358-72 e23.

26. Holfeld A, Quast JP, Bruderer R, Reiter L, de Souza N, Picotti P. Limited Proteolysis-Mass Spectrometry to Identify Metabolite-Protein Interactions. Methods Mol Biol. 2023;2554:69-89.

27. Mackmull MT, Nagel L, Sesterhenn F, Muntel J, Grossbach J, Stalder P, et al. Global, in situ analysis of the structural proteome in individuals with Parkinson's disease to identify a new class of biomarker. Nat Struct Mol Biol. 2022;29(10):978-89.

28. Reber V, Gstaiger M. Target Deconvolution by Limited Proteolysis Coupled to Mass Spectrometry. Methods Mol Biol. 2023;2706:177-90.

29. Manriquez-Sandoval E, Brewer J, Lule G, Lopez S, Fried SD. FLiPPR: A Processor for Limited Proteolysis (LiP) Mass Spectrometry Datasets Built on FragPipe. bioRxiv. 2023.

30. Gysin S, Salt M, Young A, McCormick F. Therapeutic strategies for targeting ras proteins. Genes Cancer. 2011;2(3):359-72.

31. Konstantinopoulos PA, Karamouzis MV, Papavassiliou AG. Post-translational modifications and regulation of the RAS superfamily of GTPases as anticancer targets. Nat Rev Drug Discov. 2007;6(7):541-55.

32. Busquets-Hernandez C, Triola G. Palmitoylation as a Key Regulator of Ras Localization and Function. Front Mol Biosci. 2021;8:659861.

33. Bonni A, Brunet A, West AE, Datta SR, Takasu MA, Greenberg ME. Cell survival promoted by the Ras-MAPK signaling pathway by transcription-dependent and -independent mechanisms. Science. 1999;286(5443):1358-62.

34. Li S, Couvillon AD, Brasher BB, Van Etten RA. Tyrosine phosphorylation of Grb2 by Bcr/Abl and epidermal growth factor receptor: a novel regulatory mechanism for tyrosine kinase signaling. EMBO J. 2001;20(23):6793-804.

35. Wee P, Wang Z. Epidermal Growth Factor Receptor Cell Proliferation Signaling Pathways. Cancers (Basel). 2017;9(5).

36. Killoran RC, Smith MJ. Conformational resolution of nucleotide cycling and effector interactions for multiple small GTPases determined in parallel. J Biol Chem. 2019;294(25):9937-48.

37. Takashima A, Faller DV. Targeting the RAS oncogene. Expert Opin Ther Targets. 2013;17(5):507-31.

38. Cook JH, Melloni GEM, Gulhan DC, Park PJ, Haigis KM. The origins and genetic interactions of KRAS mutations are allele- and tissue-specific. Nat Commun. 2021;12(1):1808.

39. Zeissig MN, Ashwood LM, Kondrashova O, Sutherland KD. Next batter up! Targeting cancers with KRAS-G12D mutations. Trends Cancer. 2023;9(11):955-67.

40. Sung H, Ferlay J, Siegel RL, Laversanne M, Soerjomataram I, Jemal A, et al. Global Cancer Statistics 2020: GLOBOCAN Estimates of Incidence and Mortality Worldwide for 36 Cancers in 185 Countries. CA Cancer J Clin. 2021;71(3):209-49.

41. Stickler S, Rath B, Hamilton G. Targeting KRAS in pancreatic cancer. Oncol Res. 2024;32(5):799-805.

42. Bournet B, Muscari F, Buscail C, Assenat E, Barthet M, Hammel P, et al. KRAS G12D Mutation Subtype Is A Prognostic Factor for Advanced Pancreatic Adenocarcinoma. Clin Transl Gastroenterol. 2016;7(3):e157.

43. Feng J, Hu Z, Xia X, Liu X, Lian Z, Wang H, et al. Feedback activation of EGFR/wild-type RAS signaling axis limits KRAS(G12D) inhibitor efficacy in KRAS(G12D)-mutated colorectal cancer. Oncogene. 2023;42(20):1620-33.

44. Lievre A, Bachet JB, Le Corre D, Boige V, Landi B, Emile JF, et al. KRAS mutation status is predictive of response to cetuximab therapy in colorectal cancer. Cancer Res. 2006;66(8):3992-5.

45. Van de Water J, Deininger SO, Macht M, Przybylski M, Gershwin ME. Detection of molecular determinants and epitope mapping using MALDI-TOF mass spectrometry. Clin Immun Immunpath. 1997;85:229-35.

46. Liu C, Zheng S, Wang Z, Wang S, Wang X, Yang L, et al. KRAS-G12D mutation drives immune suppression and the primary resistance of anti-PD-1/PD-L1 immunotherapy in non-small cell lung cancer. Cancer Commun (Lond). 2022;42(9):828-47.

47. Negri F, Bottarelli L, de'Angelis GL, Gnetti L. KRAS: A Druggable Target in Colon Cancer Patients. Int J Mol Sci. 2022;23(8).

48. Hillig RC, Sautier B, Schroeder J, Moosmayer D, Hilpmann A, Stegmann CM, et al. Discovery of potent SOS1 inhibitors that block RAS activation via disruption of the RAS-SOS1 interaction. Proc Natl Acad Sci U S A. 2019;116(7):2551-60.

49. Chen T, Tang X, Wang Z, Feng F, Xu C, Zhao Q, et al. Inhibition of Son of Sevenless Homologue 1 (SOS1): Promising therapeutic treatment for KRAS-mutant cancers. Eur J Med Chem. 2023;261:115828.

50. Hecht JR, Mitchell E, Neubauer MA, Burris HA, 3rd, Swanson P, Lopez T, et al. Lack of correlation between epidermal growth factor receptor status and response to Panitumumab monotherapy in metastatic colorectal cancer. Clin Cancer Res. 2010;16(7):2205-13.

51. Sorich MJ, Wiese MD, Rowland A, Kichenadasse G, McKinnon RA, Karapetis CS. Extended RAS mutations and anti-EGFR monoclonal antibody survival benefit in metastatic colorectal cancer: a meta-analysis of randomized, controlled trials. Ann Oncol. 2015;26(1):13-21.

52. Karapetis CS, Khambata-Ford S, Jonker DJ, O'Callaghan CJ, Tu D, Tebbutt NC, et al. K-ras mutations and benefit from cetuximab in advanced colorectal cancer. N Engl J Med. 2008;359(17):1757-65.

53. Temraz S, Mukherji D, Shamseddine A. Dual Inhibition of MEK and PI3K Pathway in KRAS and BRAF Mutated Colorectal Cancers. Int J Mol Sci. 2015;16(9):22976-88.

54. Muratcioglu S, Chavan TS, Freed BC, Jang H, Khavrutskii L, Freed RN, et al. GTP-Dependent K-Ras Dimerization. Structure. 2015;23(7):1325-35.

55. Nan X, Tamguney TM, Collisson EA, Lin LJ, Pitt C, Galeas J, et al. Ras-GTP dimers activate the Mitogen-Activated Protein Kinase (MAPK) pathway. Proc Natl Acad Sci U S A. 2015;112(26):7996-8001.

56. Spencer-Smith R, Koide A, Zhou Y, Eguchi RR, Sha F, Gajwani P, et al. Inhibition of RAS function through targeting an allosteric regulatory site. Nat Chem Biol. 2017;13(1):62-8.

57. Khan I, Spencer-Smith R, O'Bryan JP. Targeting the alpha4-alpha5 dimerization interface of K-RAS inhibits tumor formation in vivo. Oncogene. 2019;38(16):2984-93.

58. Ostrem JM, Peters U, Sos ML, Wells JA, Shokat KM. K-Ras(G12C) inhibitors allosterically control GTP affinity and effector interactions. Nature. 2013;503(7477):548-51.

59. Janes MR, Zhang J, Li LS, Hansen R, Peters U, Guo X, et al. Targeting KRAS Mutant Cancers with a Covalent G12C-Specific Inhibitor. Cell. 2018;172(3):578-89 e17.

60. Lanman BA, Allen JR, Allen JG, Amegadzie AK, Ashton KS, Booker SK, et al. Discovery of a Covalent Inhibitor of KRAS(G12C) (AMG 510) for the Treatment of Solid Tumors. J Med Chem. 2020;63(1):52-65.

61. Dy GK, Govindan R, Velcheti V, Falchook GS, Italiano A, Wolf J, et al. Long-Term Outcomes and Molecular Correlates of Sotorasib Efficacy in Patients With Pretreated KRAS

G12C-Mutated Non-Small-Cell Lung Cancer: 2-Year Analysis of CodeBreaK 100. J Clin Oncol. 2023;41(18):3311-7.

62. Kim D, Herdeis L, Rudolph D, Zhao Y, Bottcher J, Vides A, et al. Pan-KRAS inhibitor disables oncogenic signalling and tumour growth. Nature. 2023;619(7968):160-6.

63. Wang X, Allen S, Blake JF, Bowcut V, Briere DM, Calinisan A, et al. Identification of MRTX1133, a Noncovalent, Potent, and Selective KRAS(G12D) Inhibitor. J Med Chem. 2022;65(4):3123-33.

64. Hallin J, Bowcut V, Calinisan A, Briere DM, Hargis L, Engstrom LD, et al. Anti-tumor efficacy of a potent and selective non-covalent KRAS(G12D) inhibitor. Nat Med. 2022;28(10):2171-82.

65. Wei D, Wang L, Zuo X, Maitra A, Bresalier RS. A Small Molecule with Big Impact: MRTX1133 Targets the KRASG12D Mutation in Pancreatic Cancer. Clin Cancer Res. 2024;30(4):655-62.

66. Zheng Q, Zhang Z, Guiley KZ, Shokat KM. Strain-release alkylation of Asp12 enables mutant selective targeting of K-Ras-G12D. Nat Chem Biol. 2024;20(9):1114-22.

67. Malumbres M, Barbacid M. RAS oncogenes: the first 30 years. Nat Rev Cancer. 2003;3(6):459-65.

68. Cox AD, Fesik SW, Kimmelman AC, Luo J, Der CJ. Drugging the undruggable RAS: Mission possible? Nat Rev Drug Discov. 2014;13(11):828-51.

69. Canon J, Rex K, Saiki AY, Mohr C, Cooke K, Bagal D, et al. The clinical KRAS(G12C) inhibitor AMG 510 drives anti-tumour immunity. Nature. 2019;575(7781):217-23.

70. D'Agostino IB, Kieber JJ. The emerging family of plant response regulators. Trends Biochem. 1999;24:452-6.

71. Kakimoto T. CKI1, a histidine kinase homolog implicated in cytokinin signal transduction. Science. 1996;274:982-5.

72. Issahaku AR, Mukelabai N, Agoni C, Rudrapal M, Aldosari SM, Almalki SG, et al. Characterization of the binding of MRTX1133 as an avenue for the discovery of potential KRAS(G12D) inhibitors for cancer therapy. Sci Rep. 2022;12(1):17796.

73. Tu G, Gong Y, Yao X, Liu Q, Xue W, Zhang R. Pathways and mechanism of MRTX1133 binding to KRAS G12D elucidated by molecular dynamics simulations and Markov state models. Int J Biol Macromol. 2024;274(Pt 2):133374.

74. Liang F, Kang Z, Sun X, Chen J, Duan X, He H, et al. Inhibition mechanism of MRTX1133 on KRAS(G12D): a molecular dynamics simulation and Markov state model study. J Comput Aided Mol Des. 2023;37(3):157-66.

75. Peris-Diaz MD, Guran R, Domene C, de Los Rios V, Zitka O, Adam V, et al. An Integrated Mass Spectrometry and Molecular Dynamics Simulations Approach Reveals the Spatial Organization Impact of Metal-Binding Sites on the Stability of Metal-Depleted Metallothionein-2 Species. J Am Chem Soc. 2021;143(40):16486-501.

76. Marklund EG, Benesch JL. Weighing-up protein dynamics: the combination of native mass spectrometry and molecular dynamics simulations. Curr Opin Struct Biol. 2019;54:50-8.

77. Costeira-Paulo J, Gault J, Popova G, Ladds M, van Leeuwen IMM, Sarr M, et al. Lipids Shape the Electron Acceptor-Binding Site of the Peripheral Membrane Protein Dihydroorotate Dehydrogenase. Cell Chem Biol. 2018;25(3):309-17 e4.

78. Petrotchenko EV, Borchers CH. Protein Chemistry Combined with Mass Spectrometry for Protein Structure Determination. Chem Rev. 2022;122(8):7488-99.

79. Dixon T, MacPherson D, Mostofian B, Dauzhenka T, Lotz S, McGee D, et al. Predicting the structural basis of targeted protein degradation by integrating molecular dynamics simulations

with structural mass spectrometry. Nat Commun. 2022;13(1):5884.

80. Holderfield M. Efforts to Develop KRAS Inhibitors. Cold Spring Harb Perspect Med. 2018;8(7).